

Antisymmetric Exchange in Triangular Tricopper(II) Complexes: Correlation among Structural, Magnetic, and Electron Paramagnetic Resonance Parameters

Sacramento Ferrer,^{*,†} Francesc Lloret,^{*,‡} Emilio Pardo,[‡] Juan Modesto Clemente-Juan,[‡] Malva Liu-González,[§] and Santiago García-Granda^{||}

[†]Departament de Química Inorgànica, Universitat de València, Vicent Andrés Estellés s/n, 46100 Burjassot, Valencia, Spain

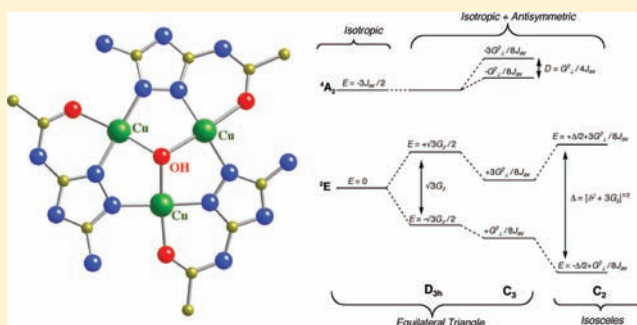
[‡]Institut de Ciència Molecular, Universitat de València, Catedràtic José Beltrán n° 2, 46980 Paterna, Valencia, Spain

[§]SCSIE-Rayos X, Universitat de València, Vicent Andrés Estellés s/n, 46100 Burjassot, Valencia, Spain

^{||}Departamento de Química Física y Analítica, Universidad de Oviedo, Julián Clavería 8, 33006 Oviedo, Spain

Supporting Information

ABSTRACT: Two new trinuclear copper(II) complexes, $[\text{Cu}_3(\mu_3\text{-OH})(\text{daat})(\text{Hdat})_2(\text{ClO}_4)_2(\text{H}_2\text{O})_3](\text{ClO}_4)_2 \cdot 2\text{H}_2\text{O}$ (**1**) and $[\text{Cu}_3(\mu_3\text{-OH})(\text{aat})_3(\text{H}_2\text{O})_3](\text{ClO}_4)_2 \cdot 3\text{H}_2\text{O}$ (**2**) (daat = 3,5-diacetyl-amino-1,2,4-triazolate, Hdat = 3,5-diamino-1,2,4-triazole, and aat = 3-acetyl-amino-5-amino-1,2,4-triazolate), have been prepared from 1,2,4-triazole derivatives and structurally characterized by X-ray crystallography. The structures of **1** and **2** consist of cationic trinuclear copper(II) complexes with a Cu_3OH core held by three N,N -triazole bridges between each pair of copper(II) atoms. The copper atoms are five-coordinate with distorted square-pyramidal geometries. The magnetic properties of **1** and **2** and those of five other related 1,2,4-triazolato tricopper(II) complexes with the same triangular structure (**3–7**) (whose crystal structures were already reported) have been investigated in the temperature range of 1.9–300 K. The formulas of **3–7** are $[\text{Cu}_3(\mu_3\text{-OH})(\text{aat})_3(\text{H}_2\text{O})_3](\text{NO}_3)_2 \cdot \text{H}_2\text{O}$ (**3**), $\{[\text{Cu}_3(\mu_3\text{-OH})(\text{aat})_3(\mu_3\text{-SO}_4)] \cdot 6\text{H}_2\text{O}\}_n$ (**4**), and $[\text{Cu}_3(\mu_3\text{-OH})(\text{aat})_3\text{A}(\text{H}_2\text{O})_2]_n \cdot x\text{H}_2\text{O}$ [$\text{A} = \text{NO}_3^-$ (**5**), CF_3SO_3^- (**6**), or ClO_4^- (**7**); $x = 0$ or 2] (aat = 3-acetyl-amino-1,2,4-triazolate). The magnetic and electron paramagnetic resonance (EPR) data have been analyzed by using the following isotropic and antisymmetric exchange Hamiltonian: $H = -J[S_1S_2 + S_2S_3] - j[S_1S_3] + G[S_1 \times S_2 + S_2 \times S_3 + S_1 \times S_3]$. **1–7** exhibit strong antiferromagnetic coupling (values for both $-J$ and $-j$ in the range of 210–142 cm^{-1}) and antisymmetric exchange (G varying from 27 to 36 cm^{-1}). At low temperatures, their EPR spectra display high-field ($g < 2.0$) signals indicating that the triangles present symmetry lower than equilateral and that the antisymmetric exchange is operative. A magneto-structural study showing a linear correlation between the Cu–O–Cu angle of the Cu_3OH core and the isotropic exchange parameters (J and j) has been conducted. Moreover, a model based on Moriya's theory that allows the prediction of the occurrence of antisymmetric exchange in the tricopper(II) triangles, via analysis of the overlap between the ground and excited states of the local Cu(II) ions, has been proposed. In addition, analytical expressions for evaluating both the isotropic and antisymmetric exchange parameters from the experimental magnetic susceptibility data of triangular complexes with local spins (S) of $1/2$, $3/2$, or $5/2$ have been purposely derived. Finally, the magnetic and EPR results of this work are discussed and compared with those of other tricopper(II) triangles reported in the literature.



INTRODUCTION

Trinuclear copper(II) complexes with trigonal symmetry have attracted significant interest because of their resemblance to the active sites of the multicopper oxidases that reduce O_2 to H_2O .^{1,2} Solomon and co-workers have studied the native system in addition to other triangular copper(II) complexes as models, and they clearly show the occurrence of strong antisymmetric exchange in all of them.³

Although $\mu_3\text{-OH}^-$ and $\mu_3\text{-O}^{2-}$ ions are the most common central bridging ligands in these compounds,⁴ some $\mu_3\text{-Cl}$,⁵

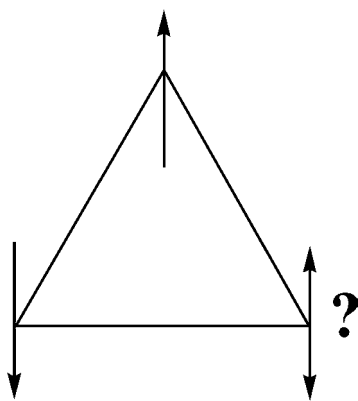
$\mu_3\text{-Br}$,⁵ and $\mu_3\text{-MeO}^{6-8}$ clusters have been described as well. The peripheral ligands that hold the M_3O core are mainly of the oxime-oximate (N,O bridge),^{9,10} Schiff base-containing derivative (O bridge),¹¹ pyrazole (N,N bridge),^{5a,12–14} or triazole (N,N bridge)^{4,15,16} type; the bridge may also belong to a macrocycle.¹⁷

Received: September 27, 2011

Published: December 23, 2011

These cyclic trinuclear metal complexes are also of interest for magnetochemists because they can be regarded as geometrically spin-frustrated systems and offer the opportunity to test magnetic exchange models.^{15,18} Geometrically frustrated antiferromagnetic compounds have attracted much attention over the past few years because of their preference for adopting unusual, even striking magnetic ground states that remain poorly understood.¹⁸ Toulouse¹⁹ is credited with introducing the general concept of magnetic frustration, a term applied to the situation in which a large fraction of magnetic sites in a lattice is subject to competing or contradictory constraints. When frustration arises purely from the geometry or topology of the lattice, then it is termed geometric frustration. The canonical example is any lattice based on equilateral triangles (Scheme 1), which depicts the situation for the three nearest-

Scheme 1



neighbor spins. The isotropic Hamiltonian for the interaction between any two spins can be written as the scalar product of the spin operators ($H = -\sum_{i,j} J_{ij} S_i S_j$); therefore, the energy is minimized for collinear (parallel or antiparallel) spin alignments. When J_{ij} is negative, which favors the antiparallel (antiferromagnetic) correlation, and J_{ij} is equal for all nearest-neighbor pairs, it is clear that only two of the three spin constraints can be satisfied simultaneously for this equilateral triangle; i.e., the system is geometrically frustrated.

The term “frustration” describes a situation in which the system cannot simultaneously satisfy all its pairwise exchange interactions and the resulting ground state can have a large degeneracy. In order to interpret the magnetic properties of these frustrated systems it is necessary to go beyond the framework of the above isotropic exchange model and to introduce an antisymmetric exchange interaction (ASE).

The exchange interactions for a pair of paramagnetic ions with spins S_A and S_B can be described in a general form as $H_{ex} = S_A \mathbf{J}_{AB} S_B$, where \mathbf{J}_{AB} is a matrix that contains the relevant exchange parameters.²⁰ This matrix can be decomposed into a scalar, J ($-J S_A S_B$ describing the isotropic exchange and generally being the dominating term), a vector, \mathbf{D}_{AB} ($S_A \mathbf{D}_{AB} S_B$ describing the anisotropic exchange), and an antisymmetric tensor, \mathbf{G}_{AB} .^{20d} The antisymmetric exchange term, which can be written as $\mathbf{G}_{AB} [S_A \times S_B]$, where \mathbf{G}_{AB} is an antisymmetric vector ($\mathbf{G}_{AB} = -\mathbf{G}_{BA}$), was introduced phenomenologically by Dzyaloshinsky to explain the weak ferromagnetism of $\alpha\text{-Fe}_2\text{O}_3$.²¹ The microscopic meaning of \mathbf{G}_{AB} was defined by Moriya.²² Therefore, this operator is usually called Dzyaloshinsky–Moriya antisymmetric interaction.

The anisotropic term, $S_A \mathbf{D}_{AB} S_B$, tends to place the spins along a given orientation in space.^{20c} The $-J S_A S_B$ term leads to parallel or antiparallel alignment of S_A and S_B (depending on the nature of the magnetic interaction, ferro or antiferromagnetic), whereas the $\mathbf{G}_{AB} [S_A \times S_B]$ term tends to arrange the spins perpendicular to each other and perpendicular to \mathbf{G}_{AB} .^{20f,23,24} These competitive interactions between these last two terms yield a nonalignment of S_A and S_B (spin canting). The canting angle, α [expressed as $\tan \alpha = G/J(6)^{1/2}$],²⁵ is in general very small because of the dominant J parameter compared with G . In fact, the antisymmetric exchange has been frequently suggested for magnetically ordered states of extended lattices where it gives rise to the phenomenon of spin canting (or weak ferromagnetism).²⁴

Moriya²² formulated rules to determine the direction of \mathbf{G}_{AB} for the different symmetries taking into account the fact that \mathbf{G}_{AB} vanishes when an inversion center is present in the A–B pair. In trigonal trinuclear complexes, the lack of a center of inversion allows a non-zero component of the antisymmetric exchange to be present in the direction normal to the metal plane. In fact, $[\text{Cu}^{\text{II}}_3]$ clusters with an equilateral triangle geometry, and equal antiferromagnetic Heisenberg exchange parameters ($J_{12} = J_{13} = J_{23} = J$) represent the simplest case of the spin-frustrated clusters and are the best candidates for the experimental observation of the Dzyaloshinsky–Moriya exchange interaction. However, information about \mathbf{G}_{AB} values for isolated complexes is very scarce.

Tsukerblat and co-workers have studied extensively the influence of antisymmetric exchange on the electronic properties of trinuclear complexes,²⁵ and they provided the first experimental observation of antisymmetric exchange in a transition metal complex.^{25b} These authors studied the trinuclear complex $[\text{Cu}_3(\mu_3\text{-OH})(\text{pyridine-2-aldoxime})_3](\text{SO}_4) \cdot 10.5\text{H}_2\text{O}$, with a trigonal symmetry, and a value of 6 cm^{-1} was obtained for G .^{25b} The second example was reported by some of us some years ago.¹⁵ We studied the ASE on two triangular complexes, $[\text{Cu}_3(\mu_3\text{-OH})(\text{aat})_3(\text{H}_2\text{O})_3](\text{NO}_3)_2 \cdot \text{H}_2\text{O}$ and $\{[\text{Cu}_3(\mu_3\text{-OH})(\text{aat})_3(\mu_3\text{-SO}_4)] \cdot 6\text{H}_2\text{O}\}_n$, and we found larger values for the G parameter ($G = 28$ and 31 cm^{-1} , respectively). The values of the G/J quotients (0.17–0.19) were significantly larger than those of Moriya’s estimation²² ($G/J \approx \Delta g/g_e \approx 0.01\text{--}0.02$).

More recently, other groups have studied the ASE in other triangles of Cu(II) and have obtained G values similar to ours. For example, Liu et al.⁶ studied the complexes $[\text{Cu}_3\text{Cl}(\mu_3\text{-OMe})(\text{Mes-Hpz})_2(\text{Mes-pz})_3]\text{Cl}$ and $[\text{Cu}_3\text{Br}(\mu_3\text{-OMe})(\text{Mes-Hpz})_2(\text{Mes-pz})_3]\text{Br}$ [$\text{Mes-Hpz} = 3,5\text{-}(2,4,6\text{-trimethylphenyl})\text{-pyrazole}$] and found G values of 33 and 47 cm^{-1} , respectively ($G/J \approx 0.17$ and 0.22 , respectively). Solomon and co-workers²⁶ studied the complex $[\text{Cu}_3(\mu\text{-OH})_3(\text{DBED})_3](\text{ClO}_4)_3$ (DBED = N,N' -di-*tert*-butylethylenediamine) and calculated a G value of 36 cm^{-1} ($G/J \approx 0.17$). These authors explained the microscopic origin of these high values of the ASE parameter (G) from the large overlap of the d functions of the neighboring Cu(II) ions in the ground and excited states due to the geometry of the metal centers. Recently, Afrati et al.⁸ reported on two more complexes, $[\text{Cu}_3(\mu_3\text{-OMe})(\text{PhPyCNO})(\text{Cl})(\text{ClO}_4)]$ and $[\text{Cu}_3(\mu_3\text{-OH})(\text{PhPyCNO})_3(2,4,5\text{-T})_2]$ (PhPyCNO = phenyl-2-pyridyl ketoxime, and 2,4,5-T = 2,4,5-trichlorophenoxyacetate), with relatively lower G values [15 and 20 cm^{-1} , respectively ($G/J \approx 0.02$ and 0.05 , respectively)].

Other triangular homo- and heterometallic complexes have also been described: $[\text{V}^{\text{IV}}_3]$,²⁷ $[\text{Cr}^{\text{III}}_3]$,²⁸ $[\text{Co}^{\text{II}}_3]$,²⁹

[Cr^{III}₂Fe^{III}],³⁰ [Fe^{III}₃],³¹ [Ni^{II}₃],³² and several other systems with different geometries.³³ Recently, Boča and Herchel have compiled the available information about the ASE parameters found for polynuclear metal complexes.^{20f}

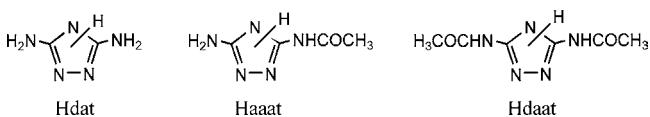
In this work, we describe the synthesis, X-ray structure, and magnetic properties of two new cyclic trimeric compounds: [Cu₃(μ₃-OH)(daat)(Hdat)₂(ClO₄)₂(H₂O)₃](ClO₄)₂·2H₂O (**1**) (daat = 3,5-diacetyl-amino-1,2,4-triazolate, and Hdat = 3,5-diamino-1,2,4-triazole) and [Cu₃(μ₃-OH)(aaat)₃(H₂O)₃](ClO₄)₂·3H₂O (**2**) (aaat = 3-acetyl-amino-5-amino-1,2,4-triazolate). Previously, some of us reported five trinuclear Cu(II) complexes of the triangular type: [Cu₃(μ₃-OH)(aaat)₃(H₂O)₃](NO₃)₂·H₂O (**3**),¹⁵ {[Cu₃(μ₃-OH)(aat)₃(μ₃-SO₄)₂·6H₂O]_n} (**4**),¹⁵ and [Cu₃(μ₃-OH)(aat)₃A(H₂O)₂·xH₂O [A = NO₃⁻ (**5**), CF₃SO₃⁻ (**6**), or ClO₄⁻ (**7**); x = 0 or 2]⁴ (aat = 3-acetyl-amino-1,2,4-triazolate). Despite the fact that their magnetic properties had already been studied, the ASE was taken into account for only two of them (**3** and **4**), and the EPR spectra were only (partially) investigated for two of them (**5**–**7**). In this respect, we have reinvestigated their magnetic properties and EPR spectra, and we analyze the results in this work. These results are discussed and compared with those found for other triangular tricopper(II) complexes previously described in the literature.

EXPERIMENTAL SECTION

Synthesis of Hdaat. The ligand Hdaat (3,5-diacetyl-amino-1,2,4-triazole) was prepared as indicated by van den Bos³⁴ and recrystallized from boiling water: mp 333 °C (lit.³⁴ 327–330 °C); FT-IR (KBr pellet) $\tilde{\nu}_{\max}$ (cm⁻¹) 3421 m, 3396 m [ν (N–H)], 1720 s [ν (C=O)], 1649 s, 1579 s [ν (C=N)/ring stretching vibrations + δ (N–H)]; ¹H NMR (DMSO-*d*₆) δ 2.0 (3H, s_b, –CH₃), 2.3 (3H, s, –CH₃), 7.5 (2H, s_b, –NHCO–), 10.2 (1H, s_b, NH_{trz}); ¹³C NMR (DMSO-*d*₆) δ 23.80 (1C, s, –CH₃), 23.95 (1C, s, –CH₃), 156.42 (2C, s, C_{trz}), 171.24 (2C, s, –CO–). Anal. Calcd for C₆H₉N₅O₂ (183.17) (%): C, 39.34; H, 4.95; N, 38.23. Found (%): C, 39.06; H, 4.98; N, 38.24.

Synthesis of [Cu₃(μ₃-OH)(daat)(Hdat)₂(ClO₄)₂(H₂O)₃](ClO₄)₂·2H₂O (1**).** A hot aqueous solution of Cu(ClO₄)₂·6H₂O (1.48 g, 4 mmol, 8 mL) was mixed with a methanolic solution of Hdaat (0.36 g, 2 mmol, 20 mL) while being continuously stirred [Cu(II):Hdaat ratio of 2:1]. The resulting green solution was allowed to stand in the freezer at 4 °C. After several months, green plate-shaped crystals of **1** (~60%) appeared together with a few blue needle-shaped crystals. Crystals of **1** were isolated on filter paper and the blue needles manually removed. One of the green plate-shaped crystals was selected for X-ray measurements. The X-ray analysis revealed that some molecules of the ligand Hdaat have suffered hydrolysis to give a ternary Hdat–daat–copper(II) compound (Schemes 2 and 3). The blue

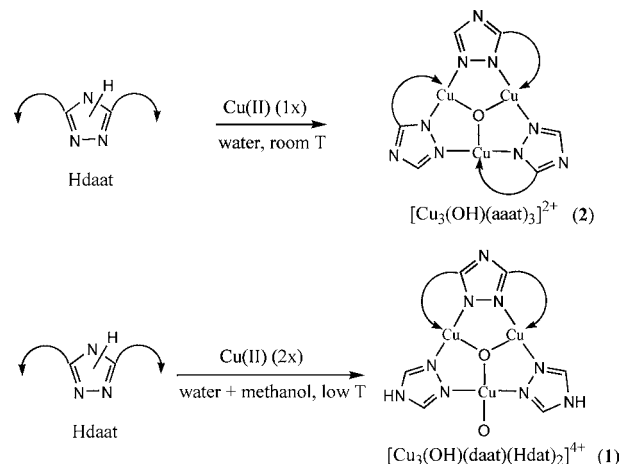
Scheme 2



needle-shaped crystals correspond to a dimeric compound {[Cu(daat)(ClO₄)(CH₃OH)]₂} (see below). For **1**: FT-IR (KBr pellet) $\tilde{\nu}_{\max}$ (cm⁻¹) 3418 m, 3300 sh [ν (O–H)_{H₂O,CH₃OH}] + ν (N–H)_{NH₂NH₂}], 1649 s [ν (C=O)], 1555 m, 1486 m [ν (C=N)/ring stretching vibrations + δ (N–H)_{NH₂NH₂}], 1145 sh, 1092 vs [ν_3 (ClO₄)], 976 vw [ν_4 (ClO₄)]. Anal. Calcd for Cu₃C₁₀N₁₅Cl₄O₂₄H₂₉ (1075.87) (%): C, 11.16; H, 2.72; N, 19.53. Found (%): C, 10.83; H, 2.81; N, 19.33.

Synthesis of [Cu₃(μ₃-OH)(aaat)₃(H₂O)₃](ClO₄)₂·3H₂O (2**).** An aqueous solution of Cu(ClO₄)₂·6H₂O (0.38 g, 1 mmol, 3 mL) was mixed with a hot aqueous solution of Hdaat (0.18 g, 1 mmol, 17 mL)

Scheme 3



while being continuously stirred [Cu(II):Hdaat ratio of 1:1]. The resulting green solution was allowed to stand at room temperature. Within ~20 days, green prismatic-shaped crystals of **2** (~70%) were observed and then manually isolated on filter paper. One of those crystals was selected for X-ray measurements. The X-ray analysis reveals that the ligand Hdaat has suffered hydrolysis, forming an aaat–copper(II) compound (Schemes 2 and 3). For **2**: FT-IR (KBr pellet) $\tilde{\nu}_{\max}$ (cm⁻¹) 3447 w, 3377 w [ν (O–H)_{H₂O}] + ν (N–H)_{NH₂NH₂}], 1630 s [ν (C=O)], 1604 s, 1508 s, 1471 w [ν (C=N)/ring stretching vibrations + δ (N–H)_{NH₂NH₂}], 1150 s, 1112 s, 1083 s [ν_3 (ClO₄)], 984 m [ν_4 (ClO₄)]. Anal. Calcd for Cu₃C₁₂N₁₅Cl₂O₁₈H₃₁ (935.04) (%): C, 15.42; H, 3.34; N, 22.47. Found (%): C, 15.64; H, 3.14; N, 22.57.

Physical Techniques. Elemental analyses were performed with a CE EA 1110 CHNS instrument. Infrared spectra were recorded with a Mattson Satellite FT-IR spectrophotometer from 4000 to 400 cm⁻¹ using KBr disks. NMR spectra were registered with a DRX 300 Bruker (300 MHz) device on DMSO-*d*₆ solutions. X-Band EPR spectra of polycrystalline samples were recorded at different temperatures with a Bruker ER 200 spectrometer equipped with a helium continuous-flow cryostat. Magnetic susceptibility measurements on polycrystalline samples were taken with a Superconducting Quantum Interference Design (SQUID) magnetometer in the temperature range of 1.9–300 K. Diamagnetic corrections of the constituent atoms were estimated from Pascal's constants. Experimental susceptibilities were also corrected for the temperature-independent paramagnetism [60×10^{-6} cm³ mol⁻¹ per copper(II)] and for the magnetization of the sample holder.

Collection and Refinement of Crystal Structure Data.

Crystallographic data for **1** and **2** are summarized in Table 1. Throughout the experiment, Mo K α (**1**) or Cu K α (**2**) radiation was used with a graphite crystal monochromator on Nonius Kappa-CCD [$\lambda = 0.71073$ Å (**1**), or $\lambda = 1.54184$ Å (**2**)] single-crystal diffractometers. Unit cell dimensions were determined from the angular settings of 7776 (**1**) and 4634 (**2**) reflections with θ between 0.998° and 27.485° (**1**) or between 3.55° and 69.40° (**2**) and refined with HKL Denzo and Scalepack.³⁵ Space groups were determined to be monoclinic *P*₂₁/*c* (**1**) or triclinic $\bar{P}1$ (**2**), from systematic absences (**1**) or from structure determination (**2**). The crystal–detector distance was fixed at 27 mm (**1**) or 29 mm (**2**), and a total of 119 (**1**) or 610 (**2**) images were collected using the oscillation method, with a scan angle per frame of 1.8° (**1**) or 2.0° (**2**) oscillation and a 300 s (**1**) or 60 s (**2**) exposure time per image. The data collection strategy was calculated with Collect.³⁶ Structure **1** was determined by using SIR97;³⁷ structure **2** was determined using DIRDIF.³⁸ Isotropic least-squares refinements on *F*² were made using SHELXL-97;³⁹ during the final stages of refinements on *F*², the positional parameters and the anisotropic thermal parameters of the non-H atoms were refined. For **2**, O4 was refined isotropically with two alternative positions with partial occupation factors of 0.696 and 0.304. For **1**, some hydrogen atoms were located by Fourier difference synthesis and

Table 1. Summary of Crystallographic Data for 1 and 2

	1	2
formula	C ₁₀ H ₂₉ Cu ₃ N ₁₅ O ₂₄ Cl ₄	C ₁₂ H ₃₁ Cu ₃ N ₁₅ O ₁₈ Cl ₂
<i>M</i> (g mol ⁻¹)	1075.90	935.07
crystal system	monoclinic	triclinic
space group	<i>P</i> 2 ₁ / <i>c</i>	<i>P</i> $\bar{1}$
<i>a</i> (Å)	11.826(5)	11.216(2)
<i>b</i> (Å)	16.272(5)	11.538(2)
<i>c</i> (Å)	18.321(5)	13.696(3)
α (deg)		76.680(11)
β (deg)	92.859(5)	69.074(11)
γ (deg)		88.280(11)
<i>V</i> (Å ³)	3521(2)	1608.3(5)
<i>Z</i>	4	2
ρ_{calc} (g cm ⁻³)	2.030	1.931
<i>F</i> (000)	2164	946
(mm ⁻¹)	2.211	4.732
<i>T</i> (K)	293(2)	293(2)
<i>R</i> ^a [<i>I</i> > 2 σ (<i>I</i>)]	0.0566	0.0882
<i>wR</i> ^b [<i>I</i> > 2 σ (<i>I</i>)]	0.1422	0.2290
<i>S</i> ^c	1.019	0.966

^a $R = \sum(|F_o| - |F_c|) / \sum|F_o|$. ^b $wR = [\sum w(|F_o| - |F_c|)^2 / \sum w|F_o|^2]^{1/2}$. ^c $S = [\sum w(|F_o| - |F_c|)^2 / (N_o - N_p)]^{1/2}$.

the rest were geometrically placed; for 2, all H atoms were geometrically placed. Figures 1 and 2, created with ORTEP,⁴⁰ show

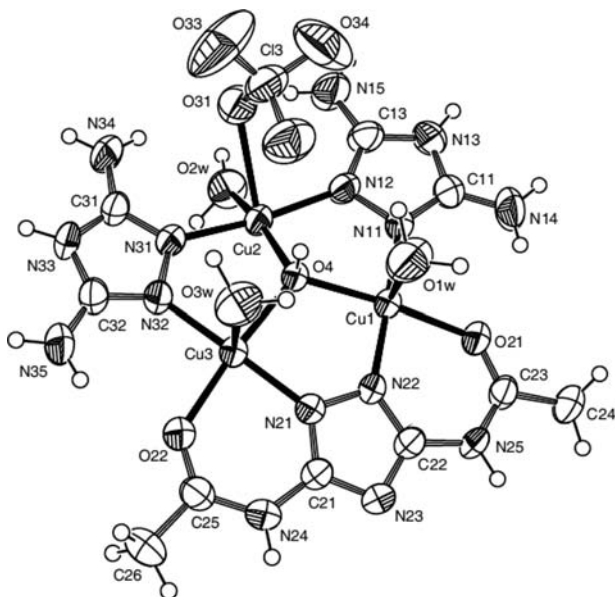


Figure 1. ORTEP plot of the Cu₃ triangle of complex 1 with the atom numbering scheme (second coordinated perchlorate not shown for the sake of clarity).

the atomic numbering schemes. Atomic scattering factors were taken from ref 41. Geometrical calculations were conducted with PARST.⁴² Crystallographic literature revision was performed with the help of CSD-Conquest.⁴³ CCDC-853895 (1) and CCDC-853896 (2) contain the supplementary crystallographic data for this paper. These data can be obtained free of charge from The Cambridge Crystallographic Data Centre (http://www.ccdc.cam.ac.uk/data_request/cif).

RESULTS AND DISCUSSION

Ligands. The 1,2,4-triazoles are versatile ligands.⁴⁴ The derivatives Haat (3-acetylamino-1,2,4-triazole), Haaat (3-acetyl-

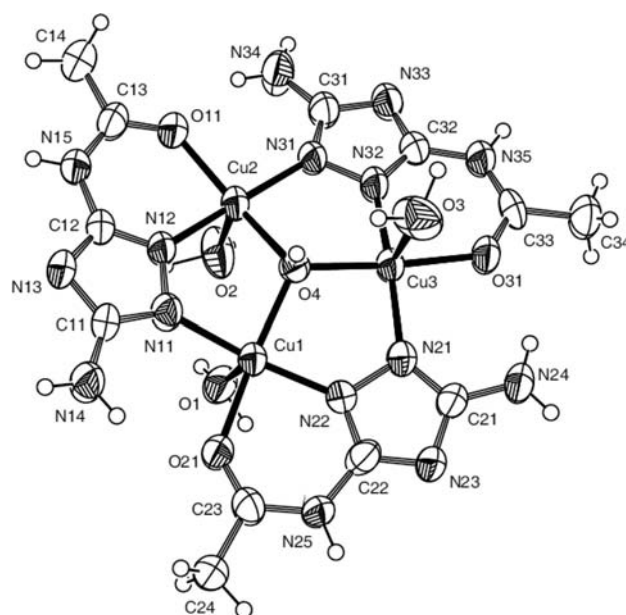


Figure 2. ORTEP plot of the Cu₃ triangle of complex 2 with the atom numbering scheme.

amino-5-amino-1,2,4-triazole), and Hppt [3-(2-hydroxyphenyl)-4-(phenyl)-1,2,4-triazole] after being mixed with copper(II) salts, under appropriate synthesis conditions, afford trinuclear complexes of the triangular type, i.e., [Cu₃(μ₃-OH)(aat)₃A·(H₂O)₂]·xH₂O (A = NO₃⁻, CF₃SO₃⁻, or ClO₄⁻; x = 0 or 2),⁴ {[Cu₃(μ₃-OH)(aat)₃(μ₃-SO₄)·6H₂O]_n}¹⁵ [Cu₃(μ₃-OH)(aaat)₃(H₂O)₃](NO₃)₂·H₂O,¹⁵ and [Cu₃(μ₃-OH)(hppt)₃(A)₂]·xH₂O (A = NO₃⁻, ClO₄⁻, or CF₃SO₃⁻; x = 2, 3, or 4).^{16a} This coordination behavior seems to be related to the presence of one chelating substituent at position 3, through which the triazole ligand forms six-membered chelating rings with the metal ion.^{44a} The compounds described in this paper have been prepared from an analogous ligand, Hdaat (3,5-diacetylamino-1,2,4-triazole) (Scheme 2), with two chelating substituents, which usually gives dimeric structures by reaction with M(II) salts.⁴⁵ In the two syntheses reported here, however, the presence of Cu(II) has promoted hydrolysis of one or two amide groups, resulting in triangular clusters instead (Scheme 3). In the synthesis of compound 2, [Cu₃(μ₃-OH)(aaat)₃(H₂O)₃](ClO₄)₂·3H₂O, with a Cu:L ratio of 1:1 (i.e., 1×) and at room temperature (Scheme 3), the loss of an acetyl group changes Hdaat into Haaat and, as expected, the isolated compound compares well with those obtained from initial Haaat. During the preparation of compound 1, [Cu₃(μ₃-OH)(daat)(Hdat)₂(ClO₄)₂(H₂O)₃](ClO₄)₂·2H₂O, in the presence of an excess of Cu(II) (Cu:L ratio of 2:1, i.e., 2×) and at low temperatures (Scheme 3), the hydrolysis proceeded further, producing guanazole (Hdat = 2,5-diamino-1,2,4-triazole) and giving for the first time in these systems a ternary complex. The purity of the starting ligand was established by elemental analysis and NMR study of Hdaat (see above). Synthesis of 2 from Haaat could be reproduced. Synthesis of 1 from a mixture of Hdaat and Hdat (guanazole) could not. Copper-induced amide hydrolysis has previously been described in the literature.⁴⁶

Crystal Structures of [Cu₃(μ₃-OH)(daat)(Hdat)₂(ClO₄)₂(H₂O)₃](ClO₄)₂·2H₂O (1) and [Cu₃(μ₃-OH)(aaat)₃(H₂O)₃](ClO₄)₂·3H₂O (2). The crystal structures of 1 and 2 are built from trinuclear cations, two noncoordinated perchlorate anions

per cation, and lattice water molecules. The trinuclear cationic units of **1** and **2** are depicted in Figures 1 and 2, respectively, together with the numbering scheme.

Both structures show similar triangles of Cu(II) ions, centered around a triply bridging hydroxo ligand and with three edge-bridging triazole groups. In **1**, the resulting $[\text{Cu}_3(\text{OH})\text{L}_2\text{L}']$ species presents a pseudomirror plane containing Cu(2) and O(4). For **2**, the chiral $[\text{Cu}_3(\text{OH})\text{L}_3]$ unit shows a pseudo-3-fold axis through the O–H bond of the hydroxo group (hence, crystals of **2** are racemic). The main difference between **1** and **2** arises from the different chelating properties of the ligands: **1** contains two nonchelating neutral Hdat ligands and one double-chelating deprotonated daat ligand, whereas **2** consists of only one type of ligand, aaat, monochelating and deprotonated. On the other hand, in the case of **2**, the central OH^- anion shares two alternative positions, namely, O(4) (occupancy factor of 63%) and O(4') (occupancy factor of 37%), symmetrically related by the pseudomirror plane through the three copper atoms, with deviations of 0.48(1) and $-0.33(2)$ Å for O(4) and O(4'), respectively. The least populated position, O(4'), has been removed from the ORTEP plot and from the structural calculations because both positions exhibit similar geometrical parameters. In **1**, the hydroxo O(4) atom deviates by 0.483(4) Å from the plane defined by the three copper atoms.

Relevant bond lengths and angles are listed in Table 2. The intratrimeric Cu...Cu' distances are in the ranges of 3.31–3.41 Å (average of 3.36 Å) for **1** and 3.36–3.40 Å (average of 3.38 Å) for **2**. In the pyramidal $\text{Cu}_3(\mu_3\text{-OH})$ core, the six Cu–O bond lengths range from 1.96 to 2.04 Å and the average Cu–O–Cu' angles are 114.3° (**1**) and 114.5° (**2**). As for the peripheral $\{\text{Cu}-\text{N}-\text{N}\}_3$ ring formed by the *N,N*-triazole ligands, the Cu–N distances of **1** and **2** are in the ranges of 1.89–1.96 and 1.90–1.96 Å, respectively. All these parameters are similar to those observed in related systems.⁴⁴ Interestingly, within the planar trinuclear unit of the $[\text{Cu}_3(\mu_3\text{-O})(\text{trz})_3(\text{OH})(\text{H}_2\text{O})_6]_n$ compound,^{16k} with Cu–O–Cu' angles of 120° , the Cu–N and Cu...Cu' distances are slightly longer (1.97–2.00 and 3.39 Å, respectively) whereas the Cu–O_{central} ones are, as expected, shorter (1.96 Å).

The three copper atoms of **1** and **2** [Cu(1), Cu(2), and Cu(3)] are five-coordinate with square-pyramidal (NNOO' + O") geometries. In all cases, except for Cu(2) in **1**, the four atoms constituting the basal plane are the central O atom from the hydroxo group, two triazole nitrogen atoms, and one carbonyl oxygen atom {the average distances being 1.93 Å (Cu–N) and 2.00 Å [Cu–O(carbonyl)]}. In **1**, the fourth coordination position of Cu(2) is occupied by one water oxygen atom instead of one carbonyl oxygen atom. The equatorial Cu(2)–O(2w) bond length (1.97 Å) of **1** is shorter than the Cu–O(carbonyl) bond lengths. The axial positions are occupied by two water molecules (bond lengths of 2.32 and 2.44 Å) and one perchlorate anion (bond length of 2.54 Å) [the three donor atoms are in *cis* with respect to the $\text{H}(\text{OH}^-)$ atom] (**1**) or by three water molecules (bond lengths of 2.26, 2.38, and 2.46 Å) (two are *trans*, and one is *cis*) (**2**). The values of the angles are typical of a tetragonal distortion (Table 2). In **1**, the “ τ ” indexes of Addison and Reedijk⁴⁷ for Cu(1) and Cu(3) are close to 0, which is the value of an ideal square pyramidal complex, whereas for Cu(2), the value is 0.10, showing that this atom has a more twisted coordination geometry (Figure S1 of the Supporting Information).

Another structural feature, potentially relevant for the magnetic properties, is the coplanarity between the basal planes

Table 2. Selected Bond Lengths (angstroms) and Angles (degrees) for **1** and **2**^a

	1	2
Cu(1)–Cu(2)	3.305(2)	3.361(2)
Cu(1)–Cu(3)	3.410(2)	3.389(2)
Cu(2)–Cu(3)	3.354(2)	3.398(2)
Cu(1)–N(11)	1.927(5)	1.940(8)
Cu(1)–N(22)	1.892(5)	1.903(7)
Cu(1)–O(21)	2.006(5)	1.984(6)
Cu(1)–O(4)	2.009(4)	2.008(9)
Cu(1)–O(1w)/O(1)	2.439(6)	2.46(1)
Cu(2)–N(12)	1.954(5)	1.919(8)
Cu(2)–N(31)	1.963(5)	1.956(8)
Cu(2)–O(2w)/O(11)	1.974(5)	1.993(6)
Cu(2)–O(4)	1.963(4)	2.043(7)
Cu(2)–O(31)/O(2)	2.541(6)	2.262(9)
Cu(3)–N(21)	1.910(5)	1.944(6)
Cu(3)–N(32)	1.948(6)	1.912(7)
Cu(3)–O(22)/O(31)	2.026(4)	2.002(7)
Cu(3)–O(4)	2.020(4)	1.983(9)
Cu(3)–O(3w)/O(3)	2.322(5)	2.379(9)
Cl(3)–O(31)	1.437(6)	
Cl(3)–O(32)	1.420(7)	
Cl(3)–O(33)	1.387(9)	
Cl(3)–O(34)	1.399(8)	
Cu(1)–O(4)–Cu(2)	112.6(2)	112.2(4)
Cu(1)–O(4)–Cu(3)	115.7(2)	116.2(5)
Cu(2)–O(4)–Cu(3)	114.7(2)	115.1(5)
N(11)–Cu(1)–O(21)	93.9(2)	96.5(3)
N(22)–Cu(1)–O(21)	86.0(2)	87.5(3)
N(22)–Cu(1)–O(4)	89.3(2)	88.4(4)
N(11)–Cu(1)–O(4)	90.6(2)	86.3(4)
N(11)–Cu(1)–O(1w)/O(1)	98.9(2)	89.2(3)
N(22)–Cu(1)–O(1w)/O(1)	88.0(2)	100.5(3)
O(21)–Cu(1)–O(1w)/O(1)	100.7(2)	84.9(3)
O(4)–Cu(1)–O(1w)/O(1)	81.3(2)	104.3(4)
N(31)–Cu(2)–O(2w)/O(11)	93.1(3)	95.1(3)
N(12)–Cu(2)–O(2w)/O(11)	91.2(2)	87.3(3)
N(12)–Cu(2)–O(4)	89.9(2)	84.9(4)
N(31)–Cu(2)–O(4)	88.8(2)	90.7(4)
N(31)–Cu(2)–O(31)/O(2)	85.9(2)	92.9(4)
O(2w)/O(11)–Cu(2)–O(31)/O(2)	85.7(2)	93.9(3)
N(12)–Cu(2)–O(31)/O(2)	84.9(2)	93.0(4)
O(4)–Cu(2)–O(31)/O(2)	111.0(2)	106.4(4)
N(21)–Cu(3)–O(22)/O(31)	85.1(2)	93.6(3)
N(32)–Cu(3)–O(22)/O(31)	96.4(2)	87.4(3)
N(32)–Cu(3)–O(4)	89.7(2)	89.7(4)
N(21)–Cu(3)–O(4)	88.9(2)	90.2(3)
N(21)–Cu(3)–O(3w)/O(3)	95.8(2)	93.2(4)
O(22)/O(31)–Cu(3)–O(3w)/O(3)	93.5(2)	88.5(3)
N(32)–Cu(3)–O(3w)/O(3)	93.8(2)	97.9(4)
O(4)–Cu(3)–O(3w)/O(3)	85.8(2)	87.0(4)

^aThe estimated standard deviations are given in parentheses.

of the copper atoms. The following dihedral Cu–Cu' angles were found: for **1**, $38.2(2)^\circ$, $34.9(2)^\circ$, and $17.3(3)^\circ$ (average of 29.9°); for **2**, $30.1(3)^\circ$, $16.9(2)^\circ$, and $6.3(2)^\circ$ (average of 15.2°) [if the planes are calculated with O(4') instead of O(4), the average value changes to 12.5°]. Compound **2** exhibits the lowest average dihedral (Cu–Cu') angle among the series of $\text{Cu}_3\text{N}_6(\text{OH})$ triazole-bridged trinuclear clusters studied so

far.^{4,15} In **1**, the comparatively large average dihedral angle must be a consequence of the nonchelation of Cu(2); in **2**, the large degree of coplanarity can be attributed to the presence of water as an axial ligand instead of bulkier anions, as already observed in the analogous aat–nitrate compound,¹⁵ and in contrast with the analogous aat compounds (all with one coordinated anion at apical positions).^{4,15}

In **1**, a second perchlorate anion approaches the three copper atoms, with contact distances of 2.688(8) Å [Cu(2)–O(41)], 2.827(7) Å [Cu(3)–O(42)], and 2.885(9) Å [Cu(1)–O(41)] (Figures S1 and S2). Therefore, this perchlorate ligand acts as a sort of additional bridge between the metallic centers of the trimeric unit. Arbitrarily, we considered the first interaction as semicoordinating, and therefore, it has been included in the coordination sphere of **1**. In **2**, the three copper atoms also tend to octahedral coordination through a sixth position achieved at the following semibonding/long distances: 2.95(2) Å for Cu(1)–O(2C^I) (I: $-x, -y, -z + 1$), 2.83(2) Å for Cu(2)–O(2D^{II}) (II: $x + 1, y + 1, +z$), and 3.07(1) Å for Cu(3)–O(1A^{III}) (III: $-x + 1, -y + 1, -z + 1$), where the O atoms belong to perchlorate groups (Figure S3).

Neighboring molecules in **1** and **2** interact with each other through H-bonds only, the tricopper cores in neighboring molecules being well-separated from each other. The shortest intertrimeric Cu...Cu' distances in each structure are 6.196(2) Å for Cu(1)...Cu(1'), 6.999(3) Å for Cu(1)...Cu(2'), and 7.085(2) Å for Cu(1)...Cu(3') (I: $-x + 1, -y + 1, -z + 1$; II: $-x + 1, -y + 1/2, -z + 1/2$) for **1** (Figure S2 of the Supporting Information) and 6.920(2) Å for Cu(1)...Cu(1'''), 6.976(2) Å for Cu(1)...Cu(2''), and 7.087(2) Å for Cu(1)...Cu(3''') (III: $-x + 1, -y + 1, -z + 2$; IV: $-x + 2, -y + 1, -z + 1$) for **2** (Figure S3).

Magnetic Properties of 1–7. The temperature dependence of the $\chi_M T$ product (χ_M being the magnetic susceptibility per trinuclear unit) for complex **1** is shown in Figure 3; those for complexes 2–7 are depicted in Figures S4–S9. At room temperature, the values of $\chi_M T$ are in the range of 0.7–0.8 cm³ mol⁻¹ K. These values are appreciably lower than those expected for three noninteracting $S = 1/2$ spins (~ 1.2 cm³ mol⁻¹ K). When the samples are cooled, $\chi_M T$ decreases continuously, reaching a plateau at 0.37–0.40 cm³ mol⁻¹ K between 60 and 90 K before decreasing further at lower temperatures to achieve values in the range of 0.20–0.25 cm³ mol⁻¹ K. The $\chi_M T$ values of the observed incipient “plateau” are close to that expected for an isolated $S = 1/2$ ground state with a reasonable g value ($\chi_M T \approx 0.4$ cm³ mol⁻¹ K). These curves clearly indicate that an intratrimer antiferromagnetic coupling is present. Noteworthy is the fact that the magnetic data for 2–7 are very similar.

To investigate the magnetic behavior of these trinuclear complexes, we used the isotropic Heisenberg–Dirac–van Vleck (HDVV) and the antisymmetric exchange (ASE) Hamiltonians. In this respect, it seems convenient to provide previously a brief background of their theoretical bases (see below).

Isotropic Exchange Formalism. The isotropic exchange can be described by the conventional HDVV Hamiltonian for a triangle of spin doublets ($S = 1/2$) (eq 1):

$$\hat{H}_{\text{iso}} = -J_{12}\hat{S}_1\hat{S}_2 - J_{13}\hat{S}_1\hat{S}_3 - J_{23}\hat{S}_2\hat{S}_3 \quad (1)$$

The corresponding energy levels obtained from this Hamiltonian for equilateral ($J_{12} = J_{23} = J_{13}$), isosceles ($J_{12} = J_{23} \neq J_{13}$), and

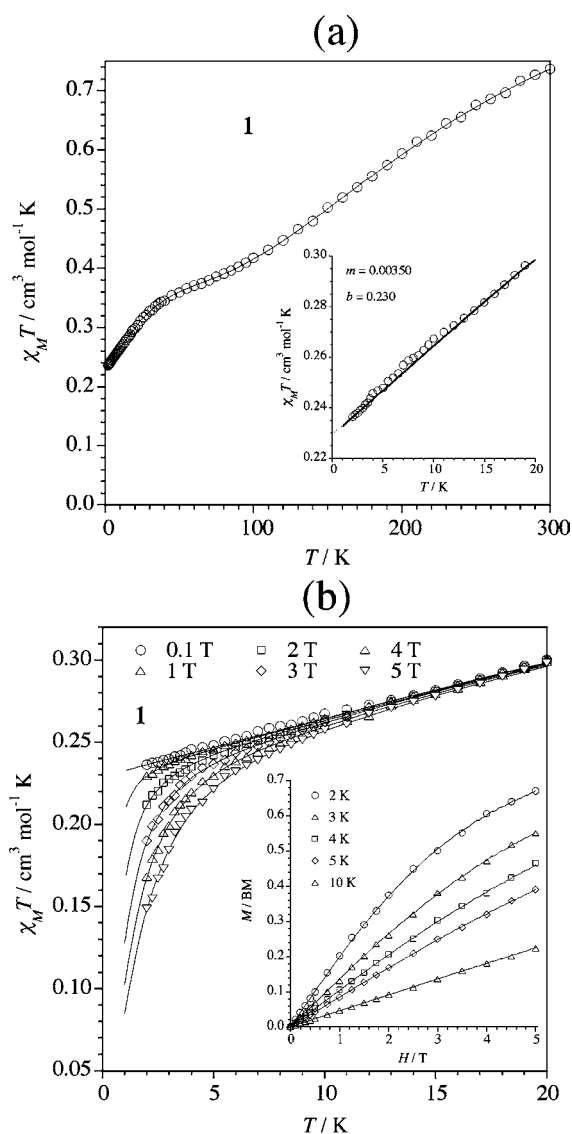


Figure 3. (a) Experimental (O) and calculated (—) $\chi_M T$ curve for **1** (χ_M being the magnetic susceptibility per trinuclear unit). The inset displays the $\chi_M T$ curve in the low-temperature region and shows the linearity expected from eqs 10 and 11. (b) Thermal dependence of $\chi_M T$ for **1** at different applied fields in the low-temperature region. The inset shows the magnetization curve at different temperatures for **1**. Solid lines represent theoretical curves (see the text).

scalene ($J_{12} \neq J_{23} \neq J_{13}$) triangles are shown in Figure 4, where some notations are introduced (eq 2):⁴⁸

$$J_{\text{av}} = (J_{12} + J_{23} + J_{13})/3 \quad (2a)$$

$$\delta = J - j \text{ where } J = J_{12} = J_{23} \text{ and } j = J_{13} \quad (2b)$$

$$\delta' = [(\Delta_1^2 + \Delta_2^2 + \Delta_3^2)/8]^{1/2} \text{ where}$$

$$\Delta_1 = J_{12} - J_{13}, \Delta_2 = J_{12} - J_{23}, \text{ and}$$

$$\Delta_3 = J_{13} - J_{23} \quad (2c)$$

The energy pattern for the equilateral triangle (C_3) includes two degenerated spin doublets, 2E , as the ground state, and a spin quadruplet, 4A , which are separated by a $3J/2$ gap. Within the framework of the isotropic HDVV model, the two

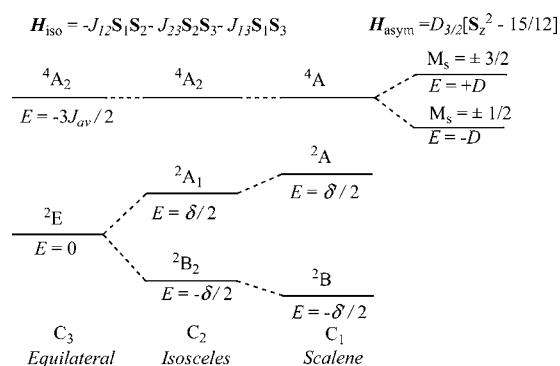


Figure 4. Energy levels for an equilateral, isosceles, and scalene triangle in the absence of antisymmetric exchange. The different notations are defined in eq 2 (see the text).

doublets in the 2E state are noninteracting and the degeneracy is accidental. Thus, the splitting of the two degenerated doublets is only possible via distortion of the C_3 symmetry, which makes nonequivalent the two (C_2) or three (C_1) J parameters. So, with weak symmetry in the presence of antiferromagnetic coupling, the low-lying spin states are a ground spin doublet (2B), an excited spin doublet (2A) at δ energy, and an excited quartet (4A) at $3J_{av}/2$ (see Figure 4). The magnetic susceptibility for such a situation may be expressed by eq 3:⁴⁸

$$\chi_M = \frac{N\beta^2 g^2}{4kT} \left[\frac{\cosh(x/2kT) + 5 \exp(3J_{av}/2kT)}{\cosh(x/2kT) + \exp(3J_{av}/2kT)} \right] \quad (3)$$

where $x = 0$ (equilateral), $x = \delta$ (isosceles), $x = \delta'$ (scalene) (see the notations in eq 2), and N , g , β , and k have their usual meanings. All the tricopper(II) compounds studied here (1–7) must be considered scalene triangles because the three Cu(II) ions in each triangle are crystallographically independent. However, it is important to point out here that for both isosceles and scalene triangles the relative energies of the three states depend only on two energy gaps that are functions of δ (or δ') and J_{av} (see Figure 4). Thus, the three interaction parameters in the scalene case (J_{ij}) cannot be determined unequivocally. In this sense, we will consider 1–7 as isosceles triangles, and from a structural point of view, the two closer Cu(II) ions will be treated as equivalent. That is, $J = J_{12} = J_{23} \neq J_{13} = j$, and $\delta = J - j$. In any case, the more relevant parameters are J_{av} and δ .

In general, it is commonly observed that, although the crystal structures of many trinuclear complexes reveal an equilateral configuration, the interpretation of the magnetic susceptibility measurements requires the adoption of the isosceles configuration, in particular at low temperatures. This observation is not surprising because the Jahn–Teller effect excludes an orbitally degenerate ground state: an internal tendency of the complex for the geometrical distortion to remove the orbital degeneracy exists. The distortion applies along the e -mode for the D_{3h} system, and an isosceles configuration arises.^{5a,49}

The magnetic behavior of equilateral, isosceles, or scalene triangles is predicted to follow a Curie law at low temperatures, when only the ground-state spin doublet (or degenerated spin doublets) is thermally populated. Specifically, at low temperatures, a plateau at $\sim 0.4 \text{ cm}^3 \text{ mol}^{-1} \text{ K}$ in the $\chi_M T$ plot is expected. That contrasts with the descending curve observed for 1–7. In fact, the experimental $\chi_M T$ curve when $T > 90 \text{ K}$ can be reproduced theoretically by using eq 3. The fit for the isosceles model is better than that of the equilateral one in all complexes

(1–7); however, some correlation among J_{av} , δ , and the g factor was not observed in all cases; consequently, these parameters could not be refined unambiguously in this high-temperature region. To choose the more realistic fit values, it is crucial to have additional data. The study of the EPR spectra together with the magnetic susceptibility at low temperature gives precious information about the magnitude of the δ parameter, allowing an unambiguous refinement of the experimental data.

As indicated above, the experimental $\chi_M T$ data below 90 K lie below the values expected for the Curie law, suggesting that other types of antiferromagnetic interactions are operative. The inclusion of an additional Weiss-like parameter, θ , which would account for possible intertrimer magnetic interactions (T replaced by $T - \theta$ in eq 3), yields values of θ too large to be realistic (values of θ between 10 and 15 K). In light of the X-ray structure determined at room temperature, intertrimer interactions are not expected to be important because of the exceedingly long and unfavorable contacts between trimers. Moreover, a very important feature is that the $\chi_M T$ data at low temperatures do not extrapolate to zero as the temperature vanishes, as could be expected for intertrimer antiferromagnetic interactions; instead, they decrease linearly and tend to a non-zero value at 0 K (see the inset of Figure 3a and Figures S4a–S9a). Hence, these large values of θ are meaningless, and the intermolecular interactions are not the factor responsible for the decrease in the $\chi_M T$ values at low temperatures.

The HDVV model serves as a reliable basis for describing exchange clusters, and it provides a correct overall picture of the spin states. Despite this fact, serious discrepancies between the predictions of the theory and experimental data are found in the low-temperature region, where the structure of individual spin levels is important (as is the anisotropy), and therefore, it is necessary to go beyond the framework of the isotropic HDVV model.

Nonisotropic Exchange Contributions. In qualitative terms and from the point of view of group theory analysis of exchange multiplets,⁵⁰ the spin quartet ($S = 3/2$) and the two degenerated spin doublets ($S = 1/2$, in the HDVV model for an equilateral triangle) correspond to the singlet 4A_2 and doublet 2E terms, respectively (assuming the D_{3h} point group) (see Figure 5). According to Kramer's theorem, the ground orbital degenerate 2E term is split, by spin–orbit interaction in first order perturbation theory, into two Kramer's doublets, E' and $[A'_1 + A'_2]$ (representations of the double group D'_3). In the second-order perturbation, multiplet 4A_2 undergoes further splitting into Kramer's doublets. Therefore, this spin–orbit coupling mixes the different states yielding an anisotropic ground state. These features can be described as an effective interaction of the antisymmetric type.^{25c} In principle, the existence of an antisymmetric exchange may yield (at low temperatures) values of the magnetic moment smaller than those expected for the Curie law in the isotropic HDVV model, which does not account for spin–orbit coupling. Another type of magnetic exchange that may reduce the magnetic moment of the ground state is biquadratic exchange,⁵¹ but for local $S_i = 1/2$ spins, it is not operative. Similarly, the asymmetric exchange, $S_A D_{AB} S_B$, is only operative for $S > 1/2$ spin states, and subsequently, it affects only the spin quartet (zero-field splitting into two Kramer's doublets, as indicated in Figure 5) but not the ground state spin doublets. In contrast, the antisymmetric exchange results in the removal of the degeneracy for these two doublets.

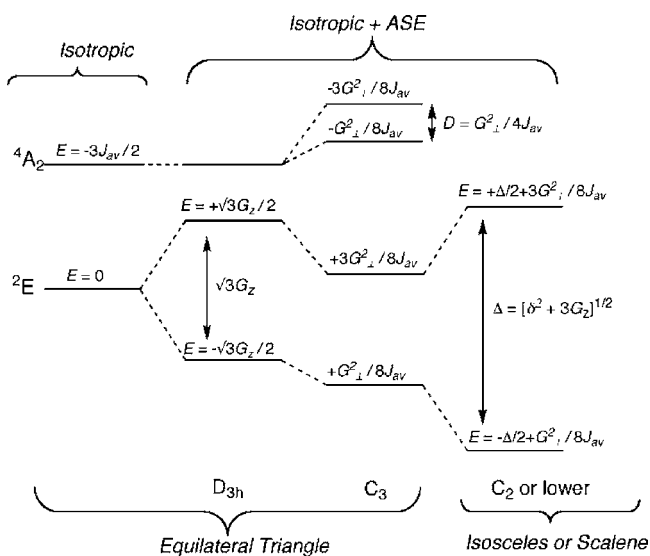


Figure 5. Energy levels for equilateral, isosceles, and scalene triangles in the presence of both isotropic and antisymmetric exchange. The different notations are defined in eqs 5 and 6 (see the text).

In summary, the orbitally degenerated ground state (2E) of the equilateral triangle complex can be further split into two Kramer's doublets, because of either the geometrically evident shift toward the weaker C_2 symmetry by the Jahn–Teller effect or the antisymmetric exchange.

Antisymmetric Exchange Interactions. The antisymmetric exchange Hamiltonian can be described by eq 4:

$$\hat{H}_{\text{ASE}} = \mathbf{G}_{12}[\hat{S}_1 \times \hat{S}_2] + \mathbf{G}_{23}[\hat{S}_2 \times \hat{S}_3] + \mathbf{G}_{31}[\hat{S}_3 \times \hat{S}_1] \quad (4)$$

where $[\hat{S}_i \times \hat{S}_j]$ and G_{ij} are the vector product and the antisymmetric vector ($\mathbf{G}_{ij} = -\mathbf{G}_{ji}$), respectively. The site symmetry of the Cu(II)–Cu(II) pair in the triangle implies a set of Moriya's conditions²² that determine possible directions of each vector, \mathbf{G}_{ij} . These conditions depend on the overall symmetry present in the triangular trimer.⁵² In an equilateral triangle (D_{3h}), each pair possesses a C_2 axis and two symmetry planes, and according to Moriya, all the \mathbf{G}_{ij} vectors have to be equal and perpendicular to the triangle plane: $\mathbf{G}_{12}^Z = \mathbf{G}_{23}^Z = \mathbf{G}_{31}^Z = \mathbf{G}_Z$. \mathbf{G}_Z is the only ASE parameter in D_{3h} symmetry ($\mathbf{G}_X = \mathbf{G}_Y = 0$). In D_3 symmetry, each pair possesses only a C_2 axis, and following Moriya's theory, the \mathbf{G}_{ij} vectors have to be perpendicular to these C_2 axes. Therefore, each \mathbf{G}_{ij} vector has two independent components: $\mathbf{G}_{12}^Z = \mathbf{G}_{23}^Z = \mathbf{G}_{31}^Z = \mathbf{G}_Z$ and $\mathbf{G}_{12}^X = \mathbf{G}_{23}^X = \mathbf{G}_{31}^X = \mathbf{G}_X$ ($\mathbf{G}_Y = 0$). For C_{3v} symmetry, each pair has only one plane, perpendicular to the Cu–Cu bond, and the \mathbf{G}_{ij} vectors must be placed in those planes. Thus, the non-zero components of \mathbf{G}_{ij} are as follows: $\mathbf{G}_{12}^Z = \mathbf{G}_{23}^Z = \mathbf{G}_{31}^Z = \mathbf{G}_Z$ and $\mathbf{G}_{12}^Y = \mathbf{G}_{23}^Y = \mathbf{G}_{31}^Y = \mathbf{G}_Y$ ($\mathbf{G}_X = 0$). In C_3 symmetry, no restrictions exist and all the components of \mathbf{G}_{ij} are non-zero ($\mathbf{G}_X \neq 0$, $\mathbf{G}_Y \neq 0$, and $\mathbf{G}_Z \neq 0$). In an isosceles triangle (C_2 point group), $\mathbf{G}_{12}^u = \mathbf{G}_{23}^u \neq \mathbf{G}_{31}^u$ (u being X , Y , or Z), and six different parameters have to be determined. Finally, in a scalene triangle, $\mathbf{G}_{12}^u \neq \mathbf{G}_{23}^u \neq \mathbf{G}_{31}^u$ and nine independent parameters exist.

With all these considerations, it becomes clear that the weak symmetry yields an enormous overparametrization, in such a way that the unambiguous determination of these parameters is not possible because they are highly correlated. Although 1–7

contain scalene triangles, the Cu(II) ions and their structural parameters are quite similar; thus, we will consider $\mathbf{G}_{12}^u = \mathbf{G}_{23}^u = \mathbf{G}_{31}^u$. With this approach, there would only be three parameters, G_Z , G_X , and G_Y . Moreover, in the particular case of complexes 1–7, parameters G_X and G_Y are very small compared to G_Z as will be shown later, and they can be neglected.

Figure 5 illustrates the energy pattern for an antiferromagnetic triangular Cu(II) trinuclear complex. The AS exchange acts within the 2E term derived from the exact Hamiltonian of the system and gives rise to two doublets. It is important to notice that the "normal" part of the AS exchange (G_Z) operates only within the basis of two "accidentally" degenerated doublets; meanwhile, two "in-plane" terms of the Hamiltonian associated with parameters G_X and G_Y (the notation $G_{\perp}^2 = G_X^2 + G_Y^2$ has been introduced) lead only to a mixing of the ground-state spin doublets with the excited state spin quadruplet, which is separated from two low-lying spin doublets by the $3J_{\text{av}}/2$ energy gap.^{27b} Therefore, the excited $S = 3/2$ level shows also a zero-field splitting, but this splitting ($G_{\perp}^2/8J_{\text{av}}$) is unaffected by G_Z and represents exclusively a second-order effect.⁵³ For this reason, the zero-field splitting of the excited quadruplet is expected to be small.

If the above discussion was taken into account, the study of the magnetic properties of 1–7 could be conducted by assuming (a) an isotropic exchange for an isosceles triangle, H_{iso} ($J = J_{12} = J_{23}$, and $j = J_{13}$), (b) an axial ASE, H_{ASE} (G_Z parallel to the C_3 axis and $G_{\perp} = 0$), and (c) an axial Hamiltonian for the Zeeman interaction with g_{\parallel} ($= g_{1z} = g_{2z} = g_{3z}$) and g_{\perp} ($= g_{1x} = g_{2x} = g_{3x} = g_{1y} = g_{2y} = g_{3y}$), as indicated in eq 5:

$$H = H_{\text{iso}} + H_{\text{ASE}} + H_{\text{Zeem}} \quad (5a)$$

$$H_{\text{iso}} = -J(S_1S_2 + S_2S_3) - jS_1S_3 \quad (5b)$$

$$H_{\text{AS}} = G_Z[S_1 \times S_2 + S_2 \times S_3 + S_3 \times S_1] \quad (5c)$$

$$H_{\text{Zeem}} = g_{\parallel}\beta(S_{1Z} + S_{2Z} + S_{3Z})H_Z + g_{\perp}\beta[(S_{1X} + S_{2X} + S_{3X})H_X + (S_{1Y} + S_{2Y} + S_{3Y})H_Y] \quad (5d)$$

In this axial model, both the ASE and Zeeman interactions do not mix the ground-state spin doublets with the excited state spin quartet and the energy expressions for the energy levels can be found by the exact diagonalization of the Hamiltonian (eq 5).^{25a}

$$E(S = 1/2, H \parallel C_3) = \pm 1/2(\Delta \pm g_{\parallel}\beta H) \quad (6a)$$

$$E(S = 1/2, H \perp C_3) = \pm 1/2(\Delta^2 + g_{\perp}^2\beta^2H^2 \pm g_{\perp}\beta H\delta)^{1/2} \quad (6b)$$

$$E(S = 3/2, H \parallel \text{or} \perp C_3) = -3J_{\text{av}}/2 + g_u\beta H M_S \quad (6c)$$

($u = z$ or xy , and $M_S = \pm 1/2, \pm 3/2$)

$$\text{where } \Delta = (\delta^2 + 3G_Z^2)^{1/2},$$

$$J_{\text{av}} = (2J + j)/3, \text{ and } \delta = J - j \quad (6d)$$

In the low-field limit ($H \ll \Delta$), eq 6b can be reduced to eq 6e:

$$E(S = 1/2, H \perp C_3) = \pm 1/2[\Delta \pm g_{\perp} \beta H \delta + (1 - \delta^2)g_{\perp}^2 \beta^2 H^2 / 2\Delta] \quad (6e)$$

From eqs 6a–6e and van Vleck's equation, an analytical expression for the magnetic susceptibility at zero field can be derived (eq 7):

$$\chi_M^{\parallel} = \frac{N\beta^2 g_{\parallel}^2}{4kT} \left[\frac{\cosh(x) + 5 \exp(3J_{av}/2kT)}{\cosh(x) + \exp(3J_{av}/2kT)} \right] \quad (7a)$$

$$\chi_M^{\perp} = \frac{N\beta^2 g_{\perp}^2}{4kT} \left[\frac{\rho^2 \cosh(x) + 5 \exp(3J_{av}/2kT) + (1 - \rho^2) \sinh(x)/x}{\cosh(x) + \exp(3J_{av}/2kT)} \right] \quad (7b)$$

where $x = \Delta/2kT$ and $\rho = \delta/\Delta$

$$\chi_M^{av} = \frac{\chi_M^{\parallel} + 2\chi_M^{\perp}}{3} \quad (7c)$$

The magnetic susceptibility of a triangular trimer of spin doublets ($S = 1/2$) is properly described by eq 7. We have checked this equation by comparing its results with those calculated through the exact matrix diagonalization (by using MAGPACK⁵⁴). The values of magnetic susceptibility calculated with both procedures were basically the same over the whole temperature range.

This equation can be easily generalized for other triangular trimers of half-integer spins such as the well-known [Cr^{III}_3] and [Fe^{III}_3] systems with $S = 3/2$ and $5/2$ local spins, respectively (the corresponding equations are given in the Appendix).

The magnetic susceptibility for the ground-state spin doublets (eq 8) of an equilateral ($\rho = 0$) or isosceles ($\rho \neq 0$) triangle can be easily obtained by neglecting the spin-quartet contribution (i.e., $kT \ll J_{av}$):

$$\chi_M^{\parallel} = \frac{N\beta^2 g_{\parallel}^2}{4kT} \quad (8a)$$

$$\chi_M^{\perp} = \frac{N\beta^2 g_{\perp}^2 \rho^2}{4kT} + \frac{2N\beta^2 g_{\perp}^2 (1 - \rho^2)}{2\Delta} \tanh\left(\frac{\Delta}{2kT}\right) \quad (8b)$$

Some interesting facts deserve to be pointed out. (a) The parallel susceptibility (χ_M^{\parallel}) is not substantially affected by the ASE and it follows a Curie law. (b) At high temperatures ($kT \gg \Delta$), χ_{\perp} tends to the limit $\chi_M^{\perp} \rightarrow (N\beta^2 g_{\perp}^2)/(4kT)$. This limit is the same for χ_M^{\parallel} , differing only in the g factor (g_{\perp} instead of g_{\parallel}). This magnetic behavior is similar to that expected for the isotropic HDVV model in this high-temperature region (no magnetic influence of the ASE). (c) At low fields and low temperatures, however, the perpendicular susceptibility (χ_M^{\perp}), strongly affected by the ASE, consists of two parts: a Curie law with an effective g value (g_{eff}^{\perp}) and a temperature-independent paramagnetism term (TIP) (eqs 8b and 9):

$$g_{eff}^{\perp} = g_{\perp} \rho = g_{\perp} \frac{\delta}{\Delta} = g_{\perp} \frac{\delta}{(\delta^2 + 3G^2)^{1/2}} \quad (9)$$

As $\rho < 1$, then $g_{eff}^{\perp} < 2$, so χ_M^{\perp} is less magnetic than expected from the isotropic HDVV model; this fact is responsible for the decrease observed in the $\chi_M T$ curves of 1–7 at low temperatures. Therefore, we can conclude that the ASE induces anisotropy in the magnetic susceptibility that increases when δ decreases. In an equilateral triangle ($\delta = 0$), $g_{eff}^{\perp} = 0$ (i.e., χ_M^{\perp} is not magnetic, and the $\chi_M^{\perp} T$ product vanishes when T decreases). If δ is very large ($\delta \gg G$), then $\rho \rightarrow 1$, $g_{eff}^{\perp} \approx g_{\perp}$, and TIP $\rightarrow 0$ (i.e., χ_M^{\perp} follows the Curie law as expected for the isotropic model). This would be the case of linear tricopper(II) complexes.

It is important to note that, for a powdered sample, the $\chi_M^{av} T$ product (eq 7c) at low temperatures ($kT \ll \Delta$) can be described by eq 10:

$$\chi_M^{av} T = \frac{4C_{\perp}(1 - \rho^2)k}{3\Delta} T + \frac{C_{\parallel} + 2C_{\perp}\rho^2}{3} \quad (10)$$

where C_{\parallel} and C_{\perp} are the Curie constants for the parallel and perpendicular susceptibility, respectively; $C_{\parallel} = (N\beta^2 g_{\parallel}^2)/(4k)$, and $C_{\perp} = (N\beta^2 g_{\perp}^2)/(4k)$.

As indicated by eq 10, $\chi_M^{av} T$ decreases linearly with T . In this sense, a plot of the experimental values of $\chi_M^{av} T$ versus T yields a straight line whose slope (m) and intercept at the origin (b) are given by eq 11:

$$m = \frac{4C_{\perp}(1 - \rho^2)k}{3\Delta} \quad (11a)$$

$$b = \frac{C_{\parallel} + 2C_{\perp}\rho^2}{3} \quad (11b)$$

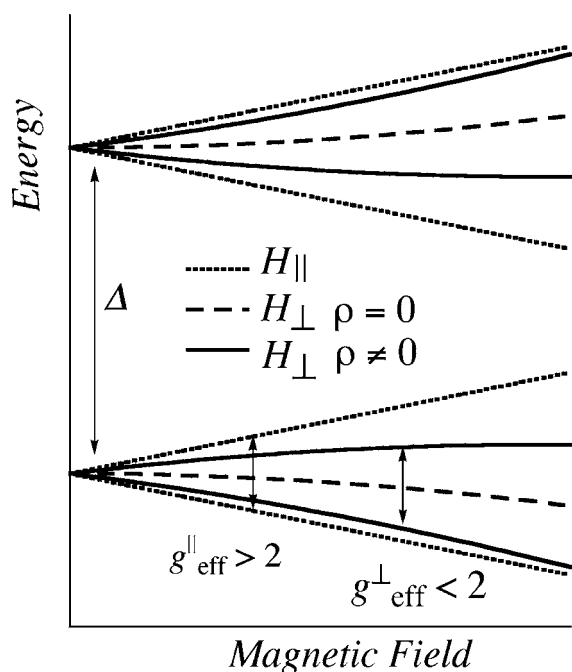
This type of plot allows the easy calculation of the values of δ and G . The insets of Figure 3a and Figures S4a–S9a show the $\chi_M T$ versus T curves at low temperatures and low fields ($H = 0.025$ T) for 1–7 and include the corresponding linear fit parameters. For 1, the fit yields m and b values of 350×10^{-5} and $0.230 \text{ cm}^3 \text{ mol}^{-1} \text{ K}$, respectively. Assuming typical values for g_{\parallel} (2.15–2.05) and g_{\perp} (2.05–2.0) and using eq 11, we found the following values for 1: $\delta = 37\text{--}41 \text{ cm}^{-1}$, and $G = 29\text{--}33 \text{ cm}^{-1}$.

To determine the more relevant magnetic parameters, J_{av} , δ , g_{\perp} , g_{\parallel} , and G_z , the thermal dependence of the magnetic susceptibility was measured in the temperature range of 2–300 K under different applied fields (0.025–5 T); magnetization measurements as a function of the magnetic field at different temperatures (2–10 K) were also performed for each compound (1–7). The results are shown in Figure 3 and Figures S4–S9 for 1–7, respectively. For each complex, different sets of measurements were analyzed as a whole (magnetization and susceptibility measurements at different fields) or separately through eq 5, with MAGPACK.⁵⁴ g_{\perp} was kept constant ($g_{\perp} = 2.0$) in the fitting process. The magnetic susceptibility measurements at low fields ($H \leq 1000$ G) were also analyzed via eq 7, and the results obtained were the same. The best-fit parameters are listed in Table 3. The theoretical curves calculated from these parameters are depicted as solid lines in the corresponding figures.

EPR Spectra of 1–7. The Zeeman effect on the ground and low-lying doublet states has been represented in Figure 6 by using eqs 6a and 6e. The dotted lines represent the Zeeman energy levels for an isosceles ($\rho \neq 0$) triangle when the applied

Table 3. Best-Fit Magnetic Parameters (energies in cm^{-1}) for 1–7

complex	$-J_{av}$	δ	G	g_{\parallel}^a
1	177.3	38	31	2.16
2	178.0	42	27	2.11
3	188.7	37	28	2.09
4	175.3	32	29	2.10
5	183.0	30	29	2.10
6	155.0	40	32	2.20
7	195.3	44	36	2.15

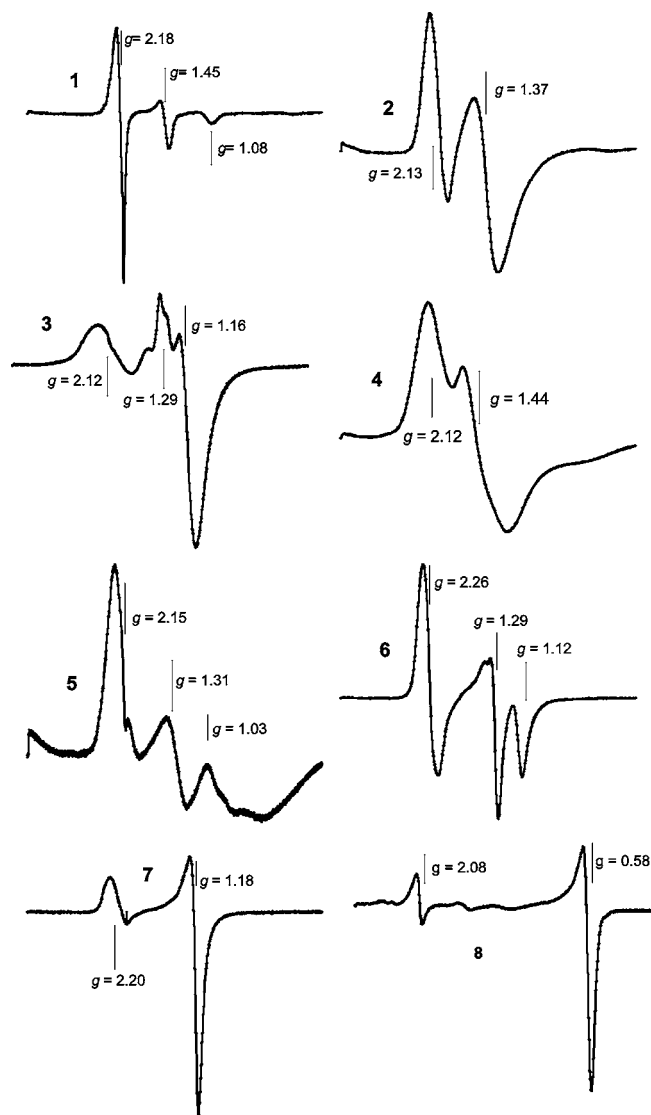
^a g_{\perp} was kept fixed at 2.0.**Figure 6.** Zeeman effect and effect of the EPR transitions on the ground and low-lying doublet states with a depiction of the origin of the low g values ($g < 2$) observed in triangular tricopper(II) complexes with antisymmetric exchange ($G \neq 0$). Parallel (···) and perpendicular (—) orientations relative to the applied magnetic field for an isosceles triangle ($\rho \neq 0$). No splitting occurs in the perpendicular orientation for an equilateral triangle (---) ($\rho = 0$) (see the text).

field is parallel, while solid lines represent the case when the field is perpendicular. In the case of a parallel field, no spin-orbit coupling between the two doublets occurs, the Zeeman energy levels vary linearly with the applied magnetic field, and $g_{\text{eff}} > 2$, which corresponds to a g_{\parallel} of the individual Cu(II) centers of the triangular Cu(II) complex. Alternatively, when the field is perpendicular, a spin-orbit coupling exists via antisymmetric exchange, the two doublets are mixed, and the Zeeman splitting is no longer linearly dependent on the field. Consequently, the Zeeman splitting is narrowed and yields an effective g value [$g_{\text{eff}}^{\perp} < 2$ (see eq 9)].

The Zeeman levels for the case of an equilateral triangle ($\rho = 0$) under a perpendicular applied field are plotted as dashed lines. In this case, the ground and low-lying doublets do not split and remain degenerate at any perpendicular field ($g_{\text{eff}}^{\perp} = 0$). Therefore, no EPR signal can be expected under these circumstances. Besides, the intradoublet transitions are

forbidden for a strict equilateral triangle.^{25a,26a,27b} Hence, the occurrence of EPR bands at $g_{\text{eff}} < 2$ indicates that the anti-symmetric exchange is operative together with a symmetry lower than that of the equilateral triangle.

Figure 7 shows the X-band EPR spectra of powdered samples of 1–7 recorded at 4.5 K. All these spectra display one band in

**Figure 7.** X-Band EPR spectra of powdered samples of 1–7 recorded at 4.5 K. For compound 8, see later and Table 4.

the 2500–3500 G field range ($g_{\text{eff}} = 2.26$ – 2.08). This band, which can be assigned to the parallel component, corresponds to the average g_{\parallel} value of the trimer local Cu(II) centers. These values are typical of $d_{x^2-y^2}$ or d_{xy} magnetic orbitals of Cu(II) ions in an axial symmetry. Compounds 2, 4, and 7 exhibit a second band at lower fields (4000–7000 G, and $g_{\text{eff}} = 1.44$ – 1.18) that corresponds to the g_{eff}^{\perp} value discussed above. In addition, the other compounds (1, 3, 5, and 6) exhibit another signal with some fine structure. All these $g_{\text{eff}} < 2$ peaks must be related to the perpendicular components and cannot be attributed to mononuclear Cu(II) impurities in the samples because of their inappropriate g values ($g_{\text{eff}} < 2$). These features are probably associated with additional transitions from the antisymmetrically coupled $S = 1/2$ spin states, which become

Table 4. Experimental Data for Antisymmetric Exchange for Triangular Tricopper(II) Complexes Antiferromagnetically Coupled (energies in cm^{-1})

compd ^a	$-J_{av}$	δ	G	Δ	ρ	$g_{ }$ (EPR)	g_{eff}^{\perp} (EPR)	g_{eff}^{\perp} (calc) ^b	β_{eg}/β_{gg} ^c	ref
1	177.3	38	31	66	0.58	2.18	1.45, 1.08	1.16	0.96	d
2	178.0	42	27	63	0.67	2.13	1.37	1.33	1.17	d
3	188.7	37	28	61	0.61	2.12	1.29, 1.16	1.22	1.21	d
4	175.3	32	29	60	0.53	2.12	1.44	1.07	1.38	d
5	183.0	30	29	58	0.51	2.15	1.31, 1.03	1.03	1.07	d
6	155.0	40	32	68	0.59	2.26	1.29, 1.12	1.18	0.80	d
7	195.3	44	36	76	0.58	2.20	1.18	1.16	0.92	d
8	400.0	22	38	69	0.32	2.08	0.58	0.64	1.18	57
A	194.0	24	33	62	0.39	2.21	1.47	0.77	0.81	6
B	210.0	63	47	103	0.61	2.19	1.52	1.22	1.18	6
C	210.0	17.5	36	64.8	0.27	2.32	≈0	0.54	0.54	26
D	800.0	30	15	39.7	0.76	2.08	1.83	1.51	0.23	8a
E	440.0	40	20	52.9	0.76	2.12	1.80	1.51	0.38	8b
F	>400	–	–	–	–	2.22	1.17	–	–	10g
G	24.5	–	≈0	–	–	2.10	1.98	–	≈0	11d
H	14.9	–	≈0	–	–	2.10	1.98	–	≈0	11d
I	25.6	–	≈0	–	–	2.18	1.91	–	≈0	11e
J	11.2	–	≈0	–	–	2.23	2.03	–	≈0	11e
K	55.0	–	≈0	–	–	2.14	1.80	–	≈0	11g
L	56.7	–	≈0	–	–	2.15	1.90	–	≈0	11g
M	44.4	–	≈0	–	–	2.15	2.0, 1.89	–	≈0	11g
N	89.9	–	≈0	–	–	2.21	2.11, 2.01	–	≈0	11g
O	216	–	≈0	–	–	2.21	2.06	–	≈0	58
P	300	–	6	–	–	–	–	–	–	25b
Q	75.0	–	5.5	–	–	2.16	2.09, 2.02	–	0.46	59
R	2.9	0.33	0.36	0.5	–	2.25	2.06	–	2.11	33c

^aA = $[\text{Cu}_3\text{Cl}(\mu_3\text{-OMe})(\text{HL})_2\text{L}_3]\text{Cl}$; HL = 3,5-(2,4,6-trimethylphenyl)pyrazole. B = $[\text{Cu}_3\text{Br}(\mu_3\text{-OMe})(\text{HL})_2\text{L}_3]\text{Br}$; HL = 3,5-(2,4,6-trimethylphenyl)pyrazole. C = $[\text{Cu}_3(\mu\text{-OH})_3\text{L}_3](\text{ClO}_4)_3$; L = *N,N'*-di-*tert*-butylethylenediamine. D = $[\text{Cu}_3(\mu_3\text{-OMe})(\text{PhPyCNO})_3(\text{Cl})(\text{ClO}_4)]$. E = $[\text{Cu}_3(\mu_3\text{-OH})(\text{PhPyCNO})_3\text{L}_2](\text{ClO}_4)_2$; L = 2,4,5-trichlorophenoxyacetate. F = $[\text{Cu}_3(\mu_3\text{-OH})(\text{O}_2\text{CR})_2(\text{py}_2\text{CNO})_3]$; R = Me, Ph. G = $[\text{Cu}_3(\mu_3\text{-OH})\text{L}_3](\text{ClO}_4)_2\cdot\text{H}_2\text{O}$; HL = 7-(ethylamino)-4-methyl-5-azahept-3-en-2-one. H = $[\text{Cu}_3(\mu_3\text{-OH})\text{L}_3](\text{ClO}_4)_2\cdot\text{H}_2\text{O}$; HL = 7-(methylamino)-4-methyl-5-azahept-3-en-2-one. I = $[\text{Cu}_3(\mu_3\text{-OH})\text{L}_3](\text{ClO}_4)_2$; L = 6-amino-3-methyl-1-phenyl-4-azahex-2-en-1-one. J = $[\text{Cu}_3(\mu_3\text{-OH})\text{L}_3](\text{ClO}_4)_2$; L = 6-amino-3,6-dimethyl-1-phenyl-4-azahex-2-en-1-one. K = $[\text{Cu}_3(\mu_3\text{-OH})\text{L}_3](\text{NO}_3)_2$; L = 8-amino-4-methyl-5-azaoct-3-en-2-one. L = $[\text{Cu}_3(\mu_3\text{-OH})\text{L}_3]_2$; L = 7-amino-4-methyl-5-azaoct-3-en-2-one. M = $[\text{Cu}_3(\mu_3\text{-OH})\text{L}_3]_2$; L = 7-amino-4-methyl-5-azahept-3-en-2-one. N = $[\text{Cu}_3(\mu_3\text{-OH})\text{L}_3][\text{Cu}^{\text{I}}\text{I}_3]$; L = 8-amino-4-methyl-5-azaoct-3-en-2-one. O = $[\text{Cu}_3(\mu_2\text{-O}_2\text{C}_{16}\text{H}_{23})_6]\cdot 1.2\text{C}_6\text{H}_{12}$. P = $[\text{Cu}_3(\mu_3\text{-OH})\text{L}_3]\text{SO}_4$; L = pyridine-2-aldoxime. Q = $[\text{Cu}_3\text{L}_3(\mu\text{-Im})_3](\text{ClO}_4)_3$. R = $\text{Na}_9[\text{Cu}_3\text{Na}_3(\text{H}_2\text{O})_9(\alpha\text{-AsW}_9\text{O}_{33})_2]$. ^bCalculated from eq 9. ^cCalculated from eq 17. ^dFrom this work.

allowed in more strongly axial or rhombic spin environments where $G_{12}^u \neq G_{23}^u \neq G_{31}^u \neq 0$ ($u = x, y, \text{ or } z$). Alternatively, these extra bands could arise from different geometric configurations or structural inhomogeneities of the triangles (e.g., from partial loss of solvent). From eq 9, we can deduce that g_{eff}^{\perp} is extremely sensitive to the $\rho = \delta/\Delta$ ratio. A relatively small variation in δ would lead to a large disparity in the g values. As discussed above, the δ parameter is expected to depend on the geometrical characteristics of the clusters. It is likely that, when the samples are cooled, several geometric configurations will be trapped, giving rise to slightly different sets of δ values.^{28b}

Table 4 lists the experimental g values obtained from EPR spectra together with those calculated from eq 9 by using the δ and G values determined from magnetic susceptibility and magnetization measurements. The table indicates that the g_{eff}^{\perp} values calculated with eq 9 (magnetic susceptibility data) compare reasonably well with those obtained from EPR spectra, although in general the calculated ones are lower. This fact has also been observed in other triangular Cu(II) complexes (see Table 4).

The EPR spectra of 1–7 are in general broad and uninformative above 50 K. When the samples are cooled, however,

several features become resolved and the intensity of the bands increases. Figure S10 shows the EPR spectra of 1–7 as a function of temperature.

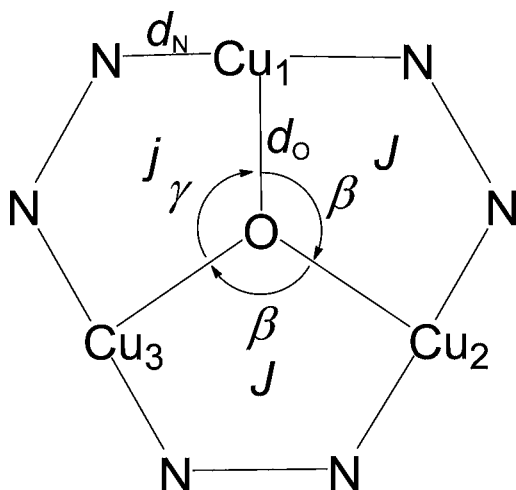
Magnetostructural Correlations. *Structural Dependence of the Isotropic Exchange.* The more relevant structural parameters (bond lengths and angles) together with the exchange parameters for complexes 1–7 are listed in Table 5. These parameters are defined in Scheme 4. The Cu–N and Cu–O bond lengths ($d_{\text{Cu-N}}$ and $d_{\text{Cu-O}}$, respectively) are the mean values for each compound. The β angle is defined by the average of the most similar Cu(1)–O–Cu(2) and Cu(1)–O–Cu(3) angles within the triangle, whereas the γ angle refers to the Cu(2)–O–Cu(3) angle (the most different one). The α_{av} angle is defined as $(2\beta + \gamma)/2$. Finally, the values of the exchange parameters are as follows: $J = J_{12} = J_{13}$, $j = J_{23}$, and $J_{av} = (2J + j)/2$. The magnetic interaction between two copper(II) ions within the triangle is mediated by both the diatomic *N,N'*-(triazole) and the monatomic *O*-(hydroxo) bridges. The structural parameters associated with the triazole bridge are comparable in the seven compounds. Except for compound 5, the other six complexes exhibit among them very similar Cu–N distances (1.92–1.94 Å). Besides, there is no relation between the variation of these parameters and the variation of those of

Table 5. Magnetostructural Data for 1–7^a

compd	$-J$ (cm ⁻¹)	β (deg)	$-j$ (cm ⁻¹)	γ (deg)	$-J_{av}$ (cm ⁻¹)	α_{av} (deg)	d_{Cu-O} (Å)	d_{Cu-N} (Å)
1	190	115.0	152	112.5	177.3	114.2	1.99	1.94
2	192	115.6	150	112.2	178.0	114.5	2.02	1.93
3	201	116.1	164	114.1	189.0	115.4	1.99	1.93
4	186	114.0	154	113.0	175.3	113.7	2.00	1.93
5	193	115.1	163	113.6	183.6	114.6	1.95	1.98
6	142	111.6	182	114.2	155.0	112.5	2.00	1.94
7	210	116.5	166	113.4	195.3	115.5	2.00	1.92

^aThe parameters are defined in Scheme 4. The distances and bond angles are average values.

Scheme 4



exchange coupling. Consequently, it can be assumed that the triazole group is a rigid bridge and that it mediates a practically constant magnetic coupling in these triangles. The hydroxo bridge also presents similar Cu–O distances (1.99–2.02 Å) in all these compounds, the only exception being compound 5, and no relation is appreciated between this small variation and the values of the exchange coupling parameters. The magnetostructural correlation involves mainly the Cu–O–Cu bridgehead angle. In this respect, as observed in Table 5, the J_{av} , J , and j parameters depend on the α , β , and γ angles, respectively: the larger the angle, the larger the magnetic coupling. So, given that $\beta > \gamma$, then $J > j$, except for compound 6, for which $\gamma > \beta$ and $j > J$. It is worth noting that the Cu–O–Cu angle is directly related with the out-of-plane shift of the hydroxo bridge from the plane defined by the copper atoms: the larger the shift, the smaller the angles. In fact, for similar compounds, it has been suggested that the more flattened the $Cu_3O(H)$ bridge (i.e., Cu–O–Cu angles closer to 120°), the stronger the magnetic interaction.^{10d} A plot of the Cu–O–Cu angle versus those of the exchange coupling constant is shown in Figure 8. The best linear fit is expressed by eq 12, where J is given in cm⁻¹.

$$J = -13.65\theta + 1383 \quad (12)$$

Significantly, the value of J varies from positive (ferromagnetic coupling) to negative (antiferromagnetic coupling) when $\theta = 101.3^\circ$. Theoretical studies of the triangular $[Cu_3(\mu_3-X)(\mu-pz)Cl_3]$ ($X = O^{2-}, Cl^-,$ or Br^- ; $pz =$ pyrazolate) copper(II) trimers have shown a magnetostructural correlation between J and the Cu–X–Cu angle, θ . The shift from ferro-

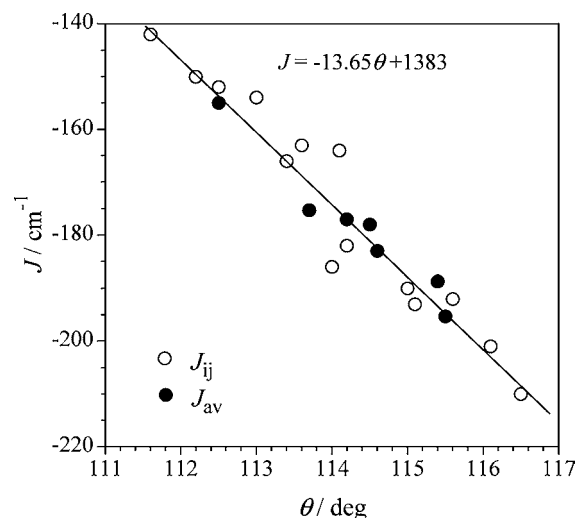


Figure 8. Linear correlation between the Cu–O–Cu angle and the exchange coupling constant. J_{ij} refers to J or j in Table 5, and $J_{av} = (2J + j)/3$. θ refers to β , γ , or α_{av} in Table 5 (see Scheme 4).

antiferromagnetic coupling was observed for θ values of 108° ($X = Cl^-$ or Br^-) and 112° ($X = O^{2-}$).⁵⁵

Although the number of examples presented herein is hardly sufficient to establish a valid correlation, it may be concluded that the Cu–O–Cu bridgehead angle is one of the main factors governing the nature and magnitude of the magnetic coupling in these triangular tricopper(II) complexes.

Orbital Dependence of the Antisymmetric Exchange. To understand the magnitude of the antisymmetric exchange parameter, G_{ij} , it is useful to consider the perturbation theory model proposed by Moriya.²² In this model, the ASE interaction between two magnetic centers, a and b , which are not related by an inversion center, is described as a second-order perturbation effect produced by a combination of local spin–orbit coupling and a superexchange interaction involving the ground states, g_a and g_b , as well as the excited states, e_a and e_b , of the two magnetic centers (eq 13):

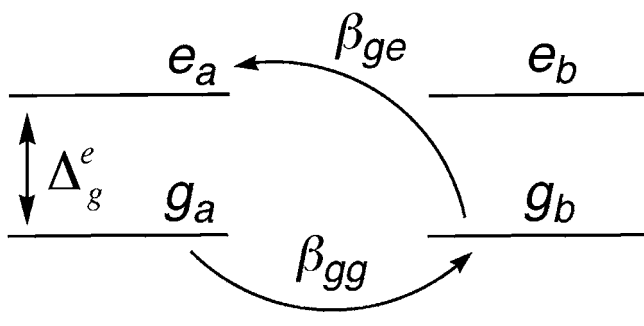
$$G_{ab}^u = - \frac{4i\lambda \langle g_a | l_u | e_a \rangle}{\Delta_g^e} J_{gg}^{ge} \quad (13)$$

where λ is the spin–orbit coupling parameter, l_u is the orbital angular momentum operator ($u = x, y,$ or z), and Δ_g^e is the energy gap between the ground g_a (or g_b) state and the excited e_a (or e_b) state. The exchange integral J_{gg}^{ge} can explicitly be written as eq 14, where 1 and 2 refer to electrons:

$$J_{gg}^{ge} = \langle g_a(1)g_b(2) | 1/r_{12} | e_a(2)g_b(1) \rangle \quad (14)$$

In eqs 13 and 14, it is assumed that $\langle g_a | l_u | e_a \rangle = \langle g_b | l_u | e_b \rangle$ and that $\langle g_a(1)g_b(2) | r_{12} | e_a(2)g_b(1) \rangle = \langle g_a(1)g_b(2) | r_{12} | g_a(2)e_b(1) \rangle$. J_{gg}^{ge} involves the transfer of the electron in the ground g_a (or g_b) state of the first magnetic center to the ground state of the second center; the electron in the ground g_b (or g_a) state of the second center is transferred to the excited e_b (or e_a) state of the first center (see Scheme 5).

Scheme 5



The J_{gg}^{ge} superexchange integral is related to the transfer integrals $\beta_{gg} = \langle g_a | l_u | g_b \rangle$ and $\beta_{ge} = \langle g_a | l_u | e_b \rangle$ as $J_{gg}^{ge} \equiv (\beta_{gg}\beta_{ge})/U$ in the same way that the isotropic superexchange integral J_{gg} described by Anderson's formalism⁵⁶ is $J_{gg} \equiv (\beta_{gg}^2/U)$, where U is the energy required to transfer an electron from g_a to g_b , thus making a polar state. Therefore, J_{gg}^{ge} and J_{gg} can be linked with the relation $J_{gg}^{ge} \equiv J_{gg}(\beta_{ge}/\beta_{gg})$, and eq 13 can be rewritten as eq 15:

$$G_{ab}^u = - \frac{4i\lambda \langle g_a | l_u | e_a \rangle}{\Delta_g^e} J_{gg} \frac{\beta_{ge}}{\beta_{gg}} \quad (15)$$

Expressions similar to eq 15 can describe each pair of Cu(II) ions belonging to a tricopper(II) triangular complex (G_{12}^u , G_{23}^u , and G_{31}^u). From the structural data of 1–7, it can be seen that the magnetic orbital of each Cu(II) center is $d_{x^2-y^2}$ ($g_a = g_b = |x^2 - y^2\rangle$), which can couple with its excited orbitals d_{xy} , d_{xz} , and d_{yz} ($e_a = e_b = |xy\rangle$, $|xz\rangle$, or $|yz\rangle$), via l_z , l_y , and l_x respectively, as indicated by eq 16:

$$\langle x^2 - y^2 | l_z | xy \rangle = 2i \quad (16a)$$

$$\langle x^2 - y^2 | l_y | xz \rangle = i \quad (16b)$$

$$\langle x^2 - y^2 | l_x | yz \rangle = i \quad (16c)$$

Figure 9 (left) shows the electron transfer between the two ground states, β_{gg} , as well as (right) between the ground state and all possible excited states, β_{ge} , allowed by spin–orbit coupling. Because of the quasi-orthogonal $d_{x^2-y^2}/d_{xz}$ and $d_{x^2-y^2}/d_{yz}$ orbital pairs, the corresponding transfer integrals are very small ($\beta_{ge} \approx 0$), so $G_{ab}^x \approx G_{ab}^y \approx 0$. Alternatively, the $d_{x^2-y^2}/d_{xz}$ and $d_{x^2-y^2}/d_{xy}$ orbital pairs form good superexchange pathways through σ -type bonds facilitated by the O-(hydroxo) bridge ($\beta_{gg} \neq 0$, and $\beta_{ge} \neq 0$), and thus, large J_{gg} and G_{ab}^z values can be expected. This analysis justifies the fact that G_{\perp} was neglected and only G_z was taken into account in describing and analyzing the magnetic properties discussed above.

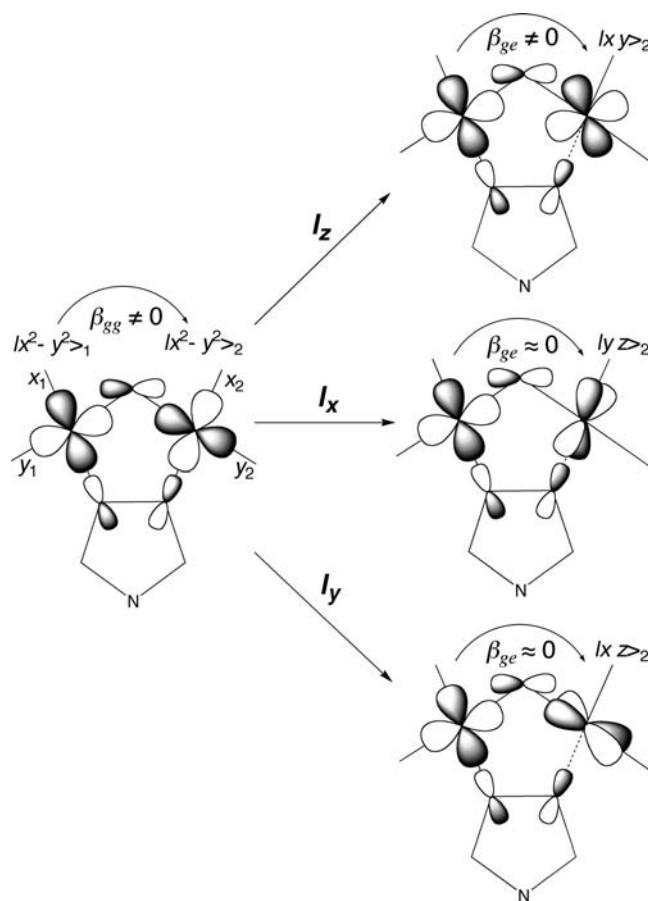


Figure 9. Spin–orbit coupling in a metal pair bridged by a hydroxo and a triazolato ligand belonging to triangular tricopper(II) complexes 1–7 as indicated by eq 16. Shown is the overlap (or electron transfer, β) between the two ground states of the two Cu(II) ions (left) and between the ground state of one Cu(II) and the excited state of the other (right) permitted by spin–orbit coupling (see the text).

It is noteworthy that $\Delta_{g_z} = (2\lambda \langle x^2 - y^2 | l_z | xy \rangle)^2 / \Delta_{x^2-y^2}^{xy} = 8\lambda / (\Delta_{x^2-y^2}^{xy})$ and that eq 15 can be rewritten as eq 17, where $\Delta_{g_z} = g_z - 2.0023$ and $J_{gg} = J_{av}$:

$$G_{ab}^z = \Delta_{g_z} J_{av} \frac{\beta_{ge}}{\beta_{gg}} \quad (17)$$

Table 4 depicts the most important isotropic and antisymmetric magnetic parameters assigned to the triangular tricopper(II) complexes whose antisymmetric exchange has been reported or discussed. From Table 4 and assuming that the three Cu(II) ions of each tricopper(II) complex are structurally equivalent (the same g_z value and $J_{gg} = J_{av}$), we can easily calculate the value for the β_{ge}/β_{gg} ratio by using eq 17. For 1–7, one obtains a β_{ge}/β_{gg} value of ≈ 1 , so $\beta_{ge} \approx \beta_{gg}$ (or $J_{gg}^{ge} \approx J_{gg}$), as could be predicted from Figure 9. The same scheme applies for compound 8 and compounds A–F if the N₃N-(triazole) bridge is changed by other bridges. In all these cases, a large antisymmetric superexchange ($J_{x^2-y^2, x^2-y^2}^{xy}$) is expected.

For compounds G–N, the antisymmetric exchange is virtually nonoperative in spite of having a relatively important magnetic coupling (J_{av}). In these complexes, the μ_3 -OH group is the only relevant bridge. Figure 10a shows the integral transfers, β_{gg} and β_{ge} , involved in the ASE. While a good superexchange

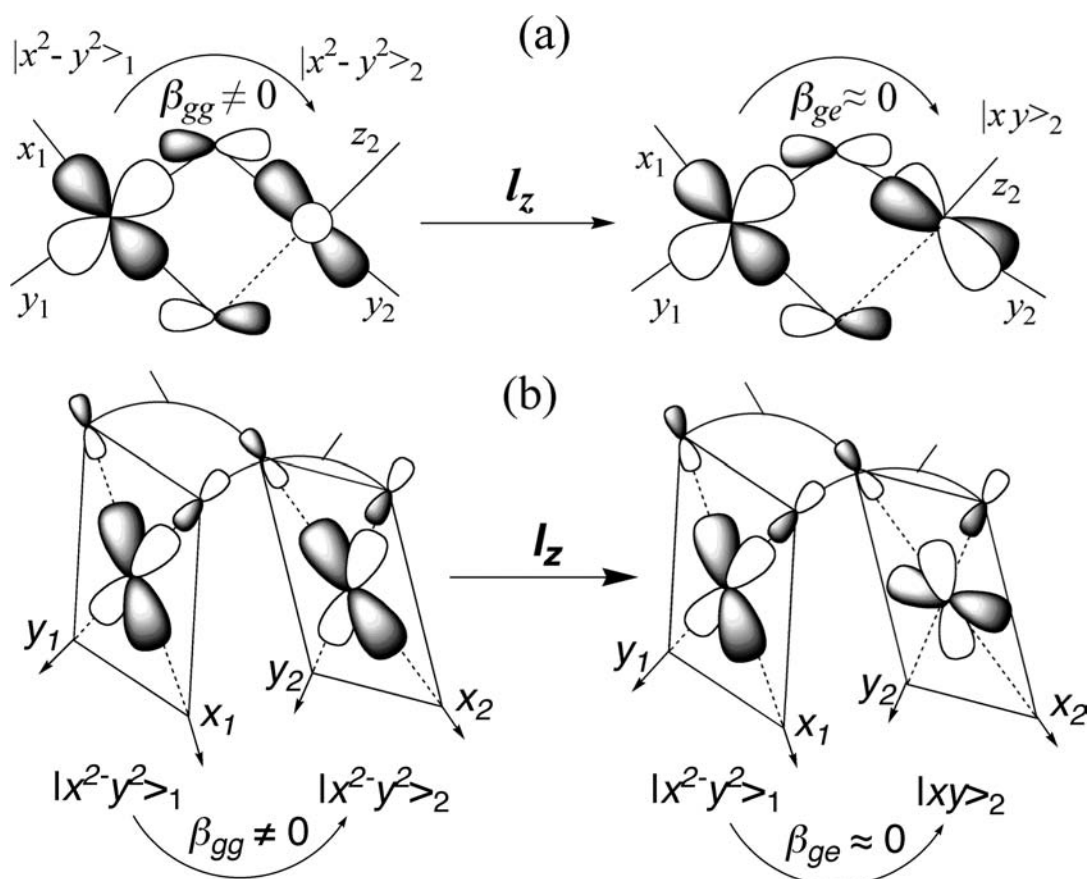


Figure 10. Spin–orbit coupling in a pair of copper(II) ions bridged by (a) a hydroxo or (b) two carboxylato ligands belonging to triangular tricopper(II) complexes **G–N** and **P**, respectively (see the text). Shown is the overlap (or electron transfer, β) between the two ground states of the two Cu(II) ions (left) and between the ground state of one Cu(II) and the excited state of the other (right) permitted by spin–orbit coupling, l_z (see the text).

pathway exists in the $d_{x^2-y^2}/d_{x^2-y^2}$ pair ($\beta_{gg} \neq 0$), the quasi-orthogonal $d_{x^2-y^2}/d_{xy}$ pair prevents any effective exchange through them ($\beta_{ge} \approx 0$); thus, $G_{ab}^z \approx 0$.

Similarly, compound **O** presents a large antiferromagnetic coupling ($J_{av} = -216 \text{ cm}^{-1}$), but no ASE has been seen in either magnetic susceptibility measurements or EPR spectra. In this triangular complex, each pair of Cu(II) ions is bridged by two *syn–syn* carboxylato groups that allow a very good exchange through the $d_{x^2-y^2}/d_{x^2-y^2}$ pair but very poor via the $d_{x^2-y^2}/d_{xy}$ pair, as shown in Figure 10b.

CONCLUSION

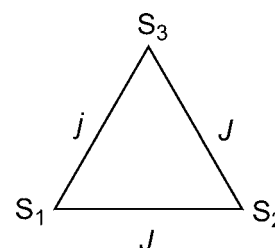
Two new trinuclear copper(II) complexes (**1** and **2**) have been prepared from 1,2,4-triazole derivatives and structurally characterized by X-ray crystallography. The magnetic properties of **1** and **2** as well as those of five other related 1,2,4-triazolato tricopper(II) complexes of the same triangular type, **3–7**, whose crystal structures were already known, have been studied. Their magnetic and EPR data have been analyzed by using an isotropic and antisymmetric exchange Hamiltonian ($H = -J[S_1S_2 + S_2S_3] - j[S_1S_3] + G[S_1 \times S_2 + S_2 \times S_3 + S_1 \times S_3]$). All these compounds exhibit strong antiferromagnetic and antisymmetric exchange. At low temperatures, their EPR spectra exhibit signals at high fields ($g < 2.0$), indicating that the antisymmetric exchange is operative together with a symmetry lower than the equilateral triangle. The magnetostructural study presented here has shown a lineal correlation between the Cu–O–Cu angle and the isotropic exchange parameters (J and j). In addition, a model based on Moriya's theory for predicting the occurrence

of antisymmetric exchange in the tricopper(II) triangles by analyzing the overlap between the ground and excited states of the local Cu(II) ions has been described. Besides, analytical expressions for evaluating both the isotropic and antisymmetric exchange parameters from the experimental magnetic susceptibility data of triangular complexes with $S = 1/2, 3/2$, or $5/2$ local spins have also been developed. Finally, all the trinuclear triangular copper(II) complexes whose structural and antisymmetric exchange parameters have been reported previously have been reviewed here, and the magnitude of the ASE in these systems has been analyzed and rationalized.

APPENDIX

Magnetic susceptibility for an equilateral ($\delta = 0$) or isosceles triangle ($\delta \neq 0$) with $S = 3/2$ or $5/2$ local spins taking into account both isotropic (eq A1) and axial antisymmetric exchange (eq A2) (Scheme 6).

Scheme 6



$$\begin{aligned}
 H_{\text{iso}} &= -J[S_1S_2 + S_2S_3] - jS_1S_3 \\
 &= -J_{\text{av}}[S_1S_2 + S_2S_3 + S_1S_3] \\
 &\quad - \frac{\delta}{3}[S_1S_2 + S_2S_3 - 2S_1S_3]
 \end{aligned} \quad (\text{A1})$$

$$H_{\text{ASE}} = G_Z[S_1 \otimes S_2 + S_2 \otimes S_3 + S_3 \otimes S_1] \quad (\text{A2})$$

where $\delta = J - j$ and $J_{\text{av}} = (2J + j)/3$.

$$\chi_{\text{M}}^{\parallel} = \frac{N\beta^2 g_{\parallel}^2}{4kT} \left[\frac{2 \cosh(D) + A}{2 \cosh(D) + B} \right] \quad (\text{A3})$$

$$\begin{aligned}
 \chi_{\text{M}}^{\perp} &= \frac{N\beta^2 g_{\perp}^2}{4kT} \\
 &\quad \left[\frac{2\rho^2 \cosh(D) + 2(1 - \rho^2) \frac{\sinh(D)}{D} + A}{2 \cosh(D) + B} \right]
 \end{aligned} \quad (\text{A4})$$

$$\chi_{\text{M}} = \frac{\chi_{\text{M}}^{\parallel} + 2\chi_{\text{M}}^{\perp}}{3} \quad (\text{A5})$$

where $x = [J_{\text{av}}/(2kT)]$, $d = [-(\delta/6kT)]$, and $D = [\Delta/(2kT)]$.

Parameters for the $S_1 = S_2 = S_3 = 3/2$ Case

$$\begin{aligned}
 \Delta &= (4\delta^2 + 48G_z)^{1/2}, \quad \rho = 2\frac{\delta}{\Delta} \\
 A &= 10E_1 \left(\sum_{i=1}^4 E_{1i} \right) + 35E_2 \left(\sum_{i=1}^3 E_{2i} \right) \\
 &\quad + 84E_3 \left(\sum_{i=1}^2 E_{3i} \right) + 165E_4 \\
 B &= 2E_1 \left(\sum_{i=1}^4 E_{1i} \right) + 3E_2 \left(\sum_{i=1}^3 E_{2i} \right) + 4E_3 \left(\sum_{i=1}^2 E_{3i} \right) \\
 &\quad + 5E_4
 \end{aligned}$$

$$\begin{aligned}
 E_1 &= e^{3x} & E_2 &= e^{8x} & E_3 &= e^{15x} & E_4 &= e^{24x} \\
 E_{11} &= e^{21d} & E_{21} &= e^{16d} & E_{31} &= e^{9d} \\
 E_{12} &= e^{3d} & E_{22} &= e^{-2d} & E_{32} &= e^{-9d} \\
 E_{13} &= e^{-9d} & E_{23} &= e^{-14d} \\
 E_{14} &= e^{-15d}
 \end{aligned}$$

Parameters for the $S_1 = S_2 = S_3 = 5/2$ Case

$$\Delta = (9\delta^2 + 243G_z)^{1/2} \text{ and } \rho = 3\frac{\delta}{\Delta}$$

$$\begin{aligned}
 A &= 10E_1 \left(\sum_{i=1}^4 E_{1i} \right) + 35E_2 \left(\sum_{i=1}^6 E_{2i} \right) \\
 &\quad + 84E_3 \left(\sum_{i=1}^5 E_{3i} \right) + 165E_4 \left(\sum_{i=1}^4 E_{4i} \right) \\
 &\quad + 286E_5 \left(\sum_{i=1}^3 E_{5i} \right) + 455E_6 \left(\sum_{i=1}^2 E_{6i} \right) + 680E_7 \\
 B &= 2E_1 \left(\sum_{i=1}^4 E_{1i} \right) + 3E_2 \left(\sum_{i=1}^6 E_{2i} \right) + 4E_3 \left(\sum_{i=1}^5 E_{3i} \right) \\
 &\quad + 5E_4 \left(\sum_{i=1}^4 E_{4i} \right) + 6E_5 \left(\sum_{i=1}^3 E_{5i} \right) + 7E_6 \left(\sum_{i=1}^2 E_{6i} \right) \\
 &\quad + 8E_7
 \end{aligned}$$

$$\begin{aligned}
 E_1 &= e^{3x} & E_2 &= e^{8x} & E_3 &= e^{15x} & E_4 &= e^{24x} & E_5 &= e^{35x} & E_6 &= e^{48x} & E_7 &= e^{63x} \\
 E_{11} &= e^{30d} & E_{21} &= e^{55d} & E_{31} &= e^{48d} & E_{41} &= e^{39d} & E_{51} &= e^{28d} & E_{61} &= e^{15d} \\
 E_{12} &= e^{6d} & E_{22} &= e^{25d} & E_{32} &= e^{18d} & E_{42} &= e^{9d} & E_{52} &= e^{-2d} & E_{62} &= e^{-15d} \\
 E_{13} &= e^{-12d} & E_{23} &= e^d & E_{33} &= e^{-6d} & E_{43} &= e^{-15d} & E_{53} &= e^{-26d} \\
 E_{14} &= e^{-24d} & E_{24} &= e^{-17d} & E_{34} &= e^{-24d} & E_{44} &= e^{-33d} \\
 E_{25} &= e^{-29d} & E_{35} &= e^{-36d} \\
 E_{26} &= e^{-35d}
 \end{aligned}$$

■ ASSOCIATED CONTENT

Supporting Information

Additional figures (S1–S10). This material is available free of charge via the Internet at <http://pubs.acs.org>.

■ AUTHOR INFORMATION

Corresponding Author

*E-mail: sacramento.ferrer@uv.es (S.F.), francisco.lloret@uv.es (F.LL.).

■ ACKNOWLEDGMENTS

This work was supported by the Ministerio de Educación y Ciencia (MEC, Spain) (Projects CTQ2007-6369/BQU, CTQ2010-15364, Consolider Ingenio CSD2007-00010) and by the Generalitat Valenciana (GV, Spain) (Projects PROM-ETEO/2009/108 and GVACOMP2011-108).

■ DEDICATION

Dedicated to Prof. Joaquín Borrás on the occasion of his retirement.

■ REFERENCES

- (1) Holm, R. H.; Solomon, E. I. *Chem. Rev.* **2004**, *104*, 347.
- (2) (a) Holm, R. H.; Kennepohl, P.; Solomon, E. I. *Chem. Rev.* **1996**, *96*, 2239. (b) Beinert, H.; Holm, R. H.; Münk, E. *Science* **1997**, *277*, 653.
- (3) (a) Solomon, E. I.; Chen, P.; Metz, M.; Lee, S.-K.; Palmer, A. E. *Angew. Chem., Int. Ed.* **2001**, *40*, 4570. (b) Lee, S.-K.; DeBeer, G. S.; Antholine, W. E.; Hedman, B.; Hodgson, K. O.; Solomon, E. I. *J. Am. Chem. Soc.* **2002**, *124*, 6180. (c) Quintanar, L.; Yon, J.; Aznar, C. P.; Palmer, A. E.; Anderson, K. K.; David Britt, R.; Solomon, E. I. *J. Am. Chem. Soc.* **2005**, *127*, 13832. (d) Yoon, J.; Mirica, L. M.; Stack, T. D. P.; Solomon, E. I. *J. Am. Chem. Soc.* **2005**, *127*, 13680. (e) Yoon, J.;

- Solomon, E. I. *Inorg. Chem.* **2005**, *44*, 8076. (f) Chalupský, J.; Neese, F.; Solomon, E. I.; Ryde, U.; Rulišek, L. *Inorg. Chem.* **2006**, *45*, 11051. (g) Yoon, J.; Solomon, E. I. *Coord. Chem. Rev.* **2007**, *251*, 379.
- (4) Ferrer, S.; Haasnoot, J. G.; Reedijk, J.; Müller, E.; Biagini-Cingi, M.; Lanfranchi, M.; Manotti-Lanfredi, A. M.; Ribas, J. *Inorg. Chem.* **2000**, *39*, 1859.
- (5) (a) Angaridis, P. A.; Baran, P.; Boca, R.; Cervantes-Lee, F.; Haase, W.; Mezei, G.; Raptis, R. G.; Werner, R. *Inorg. Chem.* **2002**, *41*, 2219. (b) Boca, R.; Dlhán, L.; Mezei, G.; Ortiz-Pérez, T.; Raptis, R. G.; Telsler, J. *Inorg. Chem.* **2003**, *42*, 5801. (c) Mezei, G.; Raptis, R. G. *Inorg. Chim. Acta* **2004**, *357*, 3279.
- (6) Liu, X.; de Miranda, M. P.; McInnes, E. J. L.; Kilner, C. A.; Halcrow, M. A. *J. Chem. Soc., Dalton Trans.* **2004**, 59.
- (7) Mezei, G.; Raptis, R. G.; Telsler, J. *Inorg. Chem.* **2006**, *45*, 8841.
- (8) (a) Afrati, T.; Dendrinou-Samara, C.; Raptopoulou, C.; Terzis, A.; Tangoulis, V.; Kessissoglou, D. P. *Dalton Trans.* **2007**, 5156. (b) Afrati, T.; Dendrinou-Samara, C.; Raptopoulou, C.; Terzis, A.; Tangoulis, V.; Tsipis, A.; Kessissoglou, D. P. *Inorg. Chem.* **2008**, *47*, 7545. (c) Afrati, T.; Pantazaki, A. A.; Dendrinou-Samara, C.; Raptopoulou, C.; Terzis, A.; Kessissoglou, D. P. *Dalton Trans.* **2010**, 39, 765.
- (9) Chaudhuri, P. *Coord. Chem. Rev.* **2003**, *241*, 143.
- (10) (a) Beckett, R.; Hoskins, B. F. *Dalton Trans.* **1972**, 291. (b) Ross, P. F.; Murmann, R. K.; Schlemper, E. O. *Acta Crystallogr.* **1974**, *B30*, 1120. (c) Baral, S.; Chakravorty, A. *Inorg. Chim. Acta* **1980**, *39*, 1. (d) Butcher, R. J.; O'Connor, C. J.; Sinn, E. *Inorg. Chem.* **1981**, *20*, 537. (e) Agnus, Y.; Louis, R.; Metz, B.; Boudon, C.; Gisselbrecht, J. P.; Gross, M. *Inorg. Chem.* **1991**, *30*, 3155. (f) Jiang, Y.-B.; Kou, H.-Z.; Wang, R.-J.; Cui, A.-L.; Ribas, J. *Inorg. Chem.* **2005**, *44*, 709. (g) Stamatatos, T. C.; Vlahopoulou, J. C.; Sanakis, Y.; Raptopoulou, C. P.; Psycharis, V.; Boudalis, A. K.; Perlepes, S. P. *Inorg. Chem. Commun.* **2006**, *9*, 814. (h) Wenzel, M.; Forgan, R. S.; Faure, A.; Mason, K.; Tasker, P. A.; Piligos, S.; Brechin, E. K.; Plieger, P. *Eur. J. Inorg. Chem.* **2009**, 4613. (i) Karmakar, S.; Das, O.; Ghosh, S.; Zangrando, E.; Johann, M.; Rentschler, E.; Weyhermüller, T.; Khanra, S.; Paine, T. K. *Dalton Trans.* **2010**, 39, 10920. (j) Maity, D.; Mukherjee, P.; Ghosh, A.; Drew, M. G. B.; Diaz, C.; Mukhopadhyay, G. *Eur. J. Inorg. Chem.* **2010**, 807.
- (11) (a) Costes, J. P.; Dahan, F.; Laurent, J. P. *Inorg. Chem.* **1986**, *25*, 413. (b) Kwiatkowski, M.; Kwiatkowski, E.; Olechnovick, D.; Ho, D. M.; Deutsch, E. *Inorg. Chim. Acta* **1988**, *150*, 65. (c) Bian, H.-D.; Xu, J.-Y.; Gu, W.; Yan, S.-P.; Cheng, P.; Liao, D.-Z.; Jiang, Z.-H. *Polyhedron* **2003**, *22*, 2927. (d) Ray, M. S.; Chattopadhyay, S.; Drew, M. G. B.; Figuerola, A.; Ribas, J.; Diaz, C.; Ghosh, A. *Eur. J. Inorg. Chem.* **2005**, 4562. (e) Sarkar, B.; Ray, M. G. B.; Drew, M. G. B.; Figuerola, A.; Diaz, C.; Ghosh, A. *Polyhedron* **2006**, *25*, 3084. (f) Sarkar, B.; Ray, M. S.; Li, Y.-Z.; Song, Y.; Figuerola, A.; Ruiz, E.; Cirera, J.; Cano, J.; Ghosh, A. *Chem.—Eur. J.* **2007**, *13*, 9297. (g) Mukherjee, P.; Drew, M. G. B.; Estrader, M.; Diaz, C.; Ghosh, A. *Inorg. Chim. Acta* **2008**, *361*, 161. (h) Rigamonti, L.; Cinti, A.; Forni, A.; Pasini, A.; Piovesana, O. *Eur. J. Inorg. Chem.* **2008**, 3633. (i) Biswas, C.; Drew, M. G. B.; Figuerola, A.; Gómez-Coca, S.; Ruiz, E.; Tangoulis, V.; Ghosh, A. *Inorg. Chim. Acta* **2010**, *363*, 846.
- (12) (a) Hulsbergen, F. B.; ten Hoedt, R. W. M.; Verschoor, J.; Reedijk, J.; Spek, A. L. *J. Chem. Soc., Dalton Trans.* **1983**, 539. (b) Angaroni, M.; Ardizzoia, G. A.; Beringhelli, T.; La Monica, G.; Gatteschi, D.; Masciocchi, N.; Moret, M. *J. Chem. Soc., Dalton Trans.* **1990**, 3305. (c) Sakai, K.; Yamada, Y.; Tsubomura, T.; Yabuki, M.; Yamaguchi, M. *Inorg. Chem.* **1996**, *35*, 522.
- (13) (a) Kamiyama, A.; Kajiwar, T.; Ito, T. *Chem. Lett.* **2002**, 980. (b) Boca, R.; Dlhán, L.; Mezei, G.; Ortiz-Pérez, T.; Gaptis, R.; Telsler, J. *Inorg. Chem.* **2003**, *42*, 5801. (c) Mezei, G.; Rivera-Carrillo, M.; Raptis, R. G. *Inorg. Chim. Acta* **2004**, *357*, 3721. (d) Casarin, M.; Corvaja, C.; di Nicola, C.; Falcomer, D.; Franco, L.; Monari, M.; Pandolfo, L.; Pettinari, C.; Piccinelli, F.; Tagliatesta, P. *Inorg. Chem.* **2004**, *43*, 5865. (e) Shen, W.-Z.; Yi, L.; Cheng, P.; Yan, S.-P.; Liao, D.-Z.; Jiang, Z.-H. *Inorg. Chem. Commun.* **2004**, *7*, 819. (f) Mezei, G.; McGrady, J. E.; Raptis, R. G. *Inorg. Chem.* **2005**, *44*, 7271. (g) Casarin, M.; Corvaja, C.; di Nicola, C.; Falcomer, D.; Franco, L.; Monari, M.; Pandolfo, L.; Pettinari, C.; Piccinelli, F. *Inorg. Chem.* **2005**, *44*, 6265.
- (14) (a) Casarin, M.; Cingolani, A.; di Nicola, C.; Falcomer, D.; Monari, M.; Pandolfo, L.; Pettinari, C. *Cryst. Growth Des.* **2007**, *7*, 676. (b) Rivera-Carrillo, M.; Chakraborty, I.; Mezei, G.; Webster, R. D.; Raptis, R. G. *Inorg. Chem.* **2008**, *47*, 7644. (c) Zhou, Q.-J.; Liu, Y.-Z.; Wang, R.-L.; Fu, J.-W.; Xu, J.-Y.; Lou, J.-S. *J. Coord. Chem.* **2009**, *62*, 311. (d) Contadi, S.; Di Nicola, C.; Garau, F.; Karabach, Y. Yu.; Martins, L. M. D. R. S.; Monari, M.; Pandolfo, L.; Pettinari, C.; Pombeiro, A. J. L. *Dalton Trans.* **2009**, 4928. (e) Rivera-Carrillo, M.; Chakraborty, I.; Raptis, R. G. *Cryst. Growth Des.* **2010**, *10*, 2606. (f) Di Nicola, C.; Garau, F.; Monari, M.; Pandolfo, L.; Pettinari, C.; Pettinari, R. *Cryst. Growth Des.* **2010**, *10*, 3120. (g) Li, H.-X.; Ren, Z.-G.; Liu, D.; Chen, Y.; Lang, J.-P.; Cheng, Z.-P.; Zhu, X.-L.; Abrahams, B. F. *Chem. Commun.* **2010**, 46, 8430.
- (15) Ferrer, S.; Lloret, F.; Bertomeu, I.; Alzuet, G.; Borrás, J.; García-Granda, S.; Liu-González, M.; Haasnoot, J. *Inorg. Chem.* **2002**, *41*, 5821.
- (16) (a) Vreugdenhil, W. Ph.D. Thesis. Leiden University, Leiden, The Netherlands, 1987. (b) Virovets, A. V.; Podberezskaya, N. V.; Lavrenova, L. G. *J. Struct. Chem.* **1997**, *38*, 532. (c) Liu, J.-C.; Guo, G.-C.; Huang, J.-S.; You, X.-Z. *Inorg. Chem.* **2003**, *42*, 235. (d) Zhou, J.-H.; Cheng, R.-M.; Song, Y.; Li, Y.-Z.; Yu, Z.; Chen, X.-T.; Xue, Z.-L.; You, X.-Z. *Inorg. Chem.* **2005**, *44*, 8011. (e) Ding, B.; Yi, L.; Cheng, P.; Liao, D.-Z.; Yan, S.-P. *Inorg. Chem.* **2006**, *45*, 5799. (f) Bichay, M.; Fronabarger, J. W.; Gilardi, R.; Butcher, R. J.; Sanborn, W. B.; Sitzmann, M. E.; Williams, M. D. *Tetrahedron Lett.* **2006**, *47*, 6663. (g) Ferrer, S.; Aznar, E.; Lloret, F.; Castiñeiras, A.; Liu-González, M. *Inorg. Chem.* **2007**, *46*, 372. (h) Lider, E. V.; Peresypkina, E. V.; Smolentsev, A. I.; Elokhina, N.; Yaroshenko, T. I.; Virovets, A. V.; Ikorskii, V. N.; Lavrenova, L. G. *Polyhedron* **2007**, *26*, 1612. (i) Ouellette, W.; Hui, Yu. M.; O'Connor, C. J.; Hagrman, D.; Zubietta, J. *Angew. Chem., Int. Ed.* **2006**, *45*, 3497. (j) Lysenko, A. B.; Govor, E. V.; Krautscheid, H.; Domasevitch, K. V. *Dalton Trans.* **2006**, 3772. (k) Zhai, Q.-G.; Lu, C.-Z.; Chen, S.-M.; Xu, X.-J.; Yang, W.-B. *Cryst. Growth Des.* **2006**, *6*, 1393. (l) Wang, Y.; Cheng, P.; Song, Y.; Liao, D.-Z.; Yan, S.-P. *Chem.—Eur. J.* **2007**, *13*, 8131. (m) Zhai, Q.; Wu, X.; Chen, S.; Chen, L.; Lu, C. *Inorg. Chim. Acta* **2007**, *360*, 3484. (n) Wu, X.-Y.; Kuang, X.-F.; Zhao, Z.-G.; Chen, S.-C.; Xie, Y.-M.; Yu, R.-M.; Lu, C.-Z. *Inorg. Chim. Acta* **2010**, *363*, 1236.
- (17) (a) Suh, M. P.; Han, M. Y.; Lee, J. H.; Min, K. S.; Hyeon, C. *J. Am. Chem. Soc.* **1998**, *120*, 3819. (b) Gonzalez-Alvarez, A.; Alfonso, I.; Cano, J.; Diaz, P.; Gotor, V.; Gotor-Fernandez, V.; Garcia-España, E.; Garcia-Granda, S.; Jimenez, H. R.; Lloret, F. *Angew. Chem.* **2009**, *48*, 6055. (c) Comarmond, J.; Dietrich, B.; Lehn, J. M.; Louis, R. J. *Chem. Soc., Chem. Commun.* **1985**, 74. (d) Mateus, P.; Delgado, R.; Lloret, F.; Cano, J.; Brandao, P.; Felix, V. *Chem.—Eur. J.* **2011**, *17*, 11193.
- (18) Greedan, J. E. *J. Mater. Chem.* **2001**, *11*, 37.
- (19) Toulouse, C. *Commun. Phys.* **1977**, *2*, 115.
- (20) (a) Heisenberg, W. *Z. Phys.* **1926**, *38*, 411. (b) Dirac, P. A. M. *Proc. R. Soc. London, Ser. A* **1929**, *123*, 714. (c) Van Vleck, J. H. *The theory of electric and magnetic susceptibility*; Oxford University Press: Oxford, U.K., 1932. (d) Bencini, A.; Gatteschi, D. *Electron Paramagnetic Resonance of Exchange Coupled Systems*; Springer-Verlag: Berlin, 1990. (e) Boca, R.; Herchel, R. *Coord. Chem. Rev.* **2004**, *248*, 757. (f) Boca, R.; Herchel, R. *Coord. Chem. Rev.* **2010**, *254*, 2973.
- (21) Dzyaloshinski, I. *J. Phys. Chem. Solids* **1958**, *4*, 241.
- (22) (a) Moriya, T. *Phys. Rev. Lett.* **1960**, *4*, 228. (b) Moriya, T. *Phys. Rev.* **1960**, *120*, 91.
- (23) Erdős, P. *J. Phys. Chem. Solids* **1966**, *27*, 1705.
- (24) Coffey, D.; Bedell, K. S.; Trugman, S. A. *Phys. Rev. B* **1990**, *42*, 6509.
- (25) (a) Tsukerblat, B. S.; Belinskii, M. I.; Fainzil'berg, V. E. *Sov. Sci. Rev., Sect. B* **1987**, *9*, 339. (b) Tsukerblat, B. S.; Kuyavskaya, B. Y.; Belinskii, M. I.; Ablov, A. V.; Novotortsev, V. M.; Kalinnikov, V. T. *Theor. Chim. Acta* **1975**, *38*, 131. (c) Tsukerblat, B. *Inorg. Chim. Acta* **2008**, *361*, 3746.

- (26) (a) Yoon, J.; Mirica, L. M.; Stack, T. D. P.; Solomon, E. I. *J. Am. Chem. Soc.* **2004**, *126*, 12586. (b) Mirica, L. M.; Stack, T. D. P. *Inorg. Chem.* **2005**, *44*, 2131.
- (27) (a) Gatteschi, D.; Sessoli, R.; Plass, W.; Müller, A.; Krickemeyer, E.; Meyer, J.; Sölter, D.; Adler, P. *Inorg. Chem.* **1996**, *35*, 1926. (b) Tsukerblat, B.; Tarantul, A.; Muller, A. *Inorg. Chem.* **2007**, *46*, 161. (c) Tsukerblat, B.; Tarantul, A.; Muller, A. *J. Chem. Phys.* **2006**, *125*, 054714. (d) Tsukerblat, B.; Tarantul, A.; Muller, A. *J. Mol. Struct.* **2007**, *838*, 124.
- (28) (a) Honda, M.; Morita, M.; Date, M. *J. Phys. Soc. Jpn.* **1992**, *61*, 3773. (b) Psycharis, V.; Raptopoulou, C. P.; Boudalis, A. K.; Sanakis, Y.; Fardis, M.; Diamantopoulos, G.; Papavassiliou, G. *Eur. J. Inorg. Chem.* **2006**, 3710. (c) Figuerola, A.; Tangoulis, V.; Ribas, J.; Hartl, H.; Brudgam, I.; Maestro, M.; Diaz, C. *Inorg. Chem.* **2007**, *46*, 11017. (d) Vlachos, A.; Psycharis, V.; Raptopoulou, C. P.; Lalioti, N.; Sanakis, Y.; Diamantopoulos, G.; Fardis, M.; Karayanni, M.; Papavassiliou, G.; Terzis, A. *Inorg. Chim. Acta* **2004**, *357*, 3162.
- (29) Berry, J. F.; Cotton, F. A.; Liu, C. Y.; Lu, T. B.; Murillo, C. A.; Tsukerblat, B. S.; Villagran, D.; Wang, X. P. *J. Am. Chem. Soc.* **2005**, *127*, 4895.
- (30) Kuyavskaya, B. Ya.; Belinskii, M. I.; Tsukerblat, B. *Sov. Phys. Solid State* **1979**, *21*, 2014.
- (31) (a) Sanakis, Y.; Macedo, A. L.; Moura, I.; Papaefthymiou, V.; Punk, E. *J. Am. Chem. Soc.* **2000**, *122*, 11855. (b) Rakitin, Y. V.; Yablokov, Y. V.; Zelentsov, V. V. *J. Magn. Reson.* **1981**, *43*, 288. (c) Boudalis, A. K.; Sanakis, Y.; Dahan, F.; Hendrich, M.; Tuchagues, J. P. *Inorg. Chem.* **2006**, *45*, 443. (d) Sanakis, Y.; Boudalis, A. K.; Tuchagues, J. P. *C. R. Chim.* **2000**, *10*, 4452. (e) Piñero, D.; Baran, P.; Boca, R.; Herchel, R.; Klein, M.; Raptis, R. G.; Renz, F.; Sanakis, Y. *Inorg. Chem.* **2007**, *46*, 10981.
- (32) Koper, P.; Mrozinski, J.; Dolezal, K.; Langer, V.; Boca, R.; Bienko, A.; Pochaba, A. *Eur. J. Inorg. Chem.* **2009**, 5475.
- (33) (a) Lines, M. E.; Ginsberg, A. P.; Martin, R. L. *Phys. Rev. Lett.* **1972**, *28*, 684. (b) Adilla, J.; Gatteschi, D.; Chaudhuri, P. *Inorg. Chim. Acta* **1997**, *260*, 217. (c) Choi, K. Y.; Matsuda, Y. H.; Nojiri, H.; Kortz, U.; Hussain, F.; Store, A. C.; Ramsey, C.; Dalal, N. S. *Phys. Rev. Lett.* **2006**, *96*, 107202. (d) Choi, K. Y.; Reyes, A. P.; Kuhns, P. L.; Mal, S. S.; Matsuda, Y. H.; Nojiri, H.; Kortz, U.; Dalal, N. S. *Phys. Rev.* **2008**, *B77*, 02406. (e) Kauffmann, K. E.; Popescu, C. V.; Dong, Y. H.; Lipscomb, J. D.; Que, L.; Munk, E. *J. Am. Chem. Soc.* **1998**, *120*, 8739. (f) Oliveira, F. T.; Bominaar, E. L.; Hirst, J.; Fee, J. A.; Munk, E. *J. Am. Chem. Soc.* **2004**, *126*, 5338. (g) Armentanao, D.; De Mundo, G.; Lloret, F.; Palii, A. V.; Julve, M. *Inorg. Chem.* **2002**, *41*, 2007. (h) Kirchner, N.; Van Slaregen, J.; Tsukerblat, B.; Waldmann, O.; Dressel, M. *Phys. Rev.* **2008**, *B78*, 094426. (i) Zueva, E. M.; Petrova, M. M.; Herchel, R.; Travnicek, Z.; Raptis, R. G.; Mathivathaan, L.; McGrady, J. E. *Dalton Trans.* **2009**, 5924.
- (34) van den Bos, B. G. *Recl. Trav. Chim. Pays-Bas* **1960**, *79*, 836.
- (35) Otwinowski, Z.; Minor, W. DENZO-SCALEPACK: Processing of X-ray Diffraction Data Collected in Oscillation Mode. In *Methods in Enzymology*, Vol. 276, Part A. *Macromolecular Crystallography*; Carter, C. W., Jr. Sweet, R. M., Eds.; Academic Press: New York, 1997.
- (36) *Collect*; Nonius BV: Delft, The Netherlands, 2000.
- (37) Altomare, A.; Burla, M. C.; Camalli, M.; Casciarano, G. L.; Giacovazzo, C.; Guagliardi, A.; Moliterni, A. G. G.; Polidori, G.; Spagna, R. *J. Appl. Crystallogr.* **1999**, *32*, 115.
- (38) Beurskens, P. T.; Beurskens, G.; Bosman, W. P.; de Gelder, R.; Garcia-Granda, S.; Gould, R. O.; Israel, R.; Smits, J. M. M. *The DIRDIF-99 program system: Technical Report of the Crystallography Laboratory*; University of Nijmegen: Nijmegen, The Netherlands, 1999.
- (39) Sheldrick, G. M. *SHELX97: Programs for Crystal Structure Analysis*, release 97-2; University of Göttingen: Göttingen, Germany, 1998.
- (40) Farrugia, L. J. *J. Appl. Crystallogr.* **1997**, *30*, 565.
- (41) Hahn, T., Ed. *International Tables for X-ray Crystallography*; Kluwer Academic Publishers: Dordrecht, The Netherlands, 1995; Vol. A.
- (42) (a) Nardelli, M. *Comput. Chem.* **1983**, *7*, 95. (b) Nardelli, M. *Comput. Chem.* **1995**, *28*, 659.
- (43) ConQuest Interface, The Cambridge Structural Database, release 5.32; Cambridge, U.K. (accessed May 2011).
- (44) (a) Haasnoot, J. G. *Coord. Chem. Rev.* **2000**, *200*, 131. (b) Klingele, M. H.; Brooker, S. *Coord. Chem. Rev.* **2003**, *241*, 119. (c) Beckmann, U.; Brooker, S. *Coord. Chem. Rev.* **2003**, *245*, 17. (d) Aromí, G.; Barrios, L.-A.; Roubeau, O.; Gamez, P. *Coord. Chem. Rev.* **2011**, *255*, 485.
- (45) (a) Ferrer, S.; van Koningsbruggen, P. J.; Haasnoot, J. G.; Reedijk, J.; Kooijman, H.; Spek, A. L.; Lezama, L.; Arif, A. M.; Miller, J. S. *J. Chem. Soc., Dalton Trans.* **1999**, 4269. (b) Ferrer, S.; Hernández-Gil, J.; Lloret, F.; Liu-González, M. Manuscript in preparation.
- (46) Driessen, W. L.; Chang, L.; Finazzo, C.; Gorter, S.; Rehorst, D.; Reedijk, J.; Lutz, M.; Spek, A. L. *Inorg. Chim. Acta* **2003**, *350*, 25.
- (47) Addison, A. W.; Rao, T. N.; Reedijk, J.; van Rijn, J.; Verschoor, G. C. *J. Chem. Soc., Dalton Trans.* **1984**, 1349.
- (48) Kahn, O. *Molecular Magnetism*; VCH Publishers: New York, 1993.
- (49) Tsukerblat, B.; Tarantul, A.; Muller, A. *J. Mol. Struct.* **2007**, *838*, 124.
- (50) Tsukerblat, B. *Inorg. Chim. Acta* **2008**, *361*, 3746.
- (51) (a) Griffith, J. S. *Struct. Bonding (Berlin, Ger.)* **1972**, *10*, 87. (b) Belinskii, M. I.; Kuyavskaya, B. Y.; Tsukerblat, B.; Ablov, A. V.; Kushkulei, L. M. *Koord. Khim.* **1976**, *2*, 1099.
- (52) Tsukerblat, B.; Tarantul, A.; Muller, A. *Phys. Lett. A* **2006**, *353*, 48.
- (53) Belinsky, M. I. *Inorg. Chem.* **2008**, *47*, 3521.
- (54) Borrás-Almenar, J. J.; Clemente-Juan, J. M.; Coronado, E.; Tsukerblat, B. *J. Comput. Chem.* **2001**, *22*, 985.
- (55) Wang, L.-L.; Sun, Y.-M.; Yu, Z.-Y.; Qi, Z.-N.; Liu, C.-B. *J. Phys. Chem. A* **2009**, *113*, 10534.
- (56) Anderson, P. W. *Phys. Rev.* **1959**, *115*, 2.
- (57) **8** is $[\text{Cu}_3(\mu_3\text{-O})\text{L}_3]\text{ClO}_4$ (L is the acetone azine of diacetyl hydrazone oxime). (a) Datta, D.; Aliaga, N.; Lloret, F. Manuscript in preparation. (b) Chakrabarti, P.; Puranik, V. G.; Naskar, J. P.; Hati, S.; Datta, D. *Indian J. Chem.* **2000**, *39*, 571.
- (58) Cage, B.; Cotton, F. A.; Dalal, N. S.; Hilard, E. A.; Rakvin, B.; Ramsey, C. M. *J. Am. Chem. Soc.* **2003**, *125*, 59.
- (59) Padilla, J.; Gatteschi, D.; Chaudhuri, P. *Inorg. Chim. Acta* **1997**, *260*, 217.